

Main revisions and response to reviewers' comments

Manuscript No.: acp-2016-567

Title: Development of a high-resolution emission inventory and its evaluation and application through air quality modeling for Jiangsu Province, China

Authors: Yaduan Zhou, Yu Zhao, Pan Mao, Qiang Zhang, Jie Zhang, Qiu Liping, Yang Yang

We thank very much for the valuable comments and suggestions from the two reviewers, which help us improve our manuscript. The comments were carefully considered and revisions have been made in response to suggestions. Following is our point-by-point responses to the comments and corresponding revisions.

Reviewer #1

1. General comments: This paper presents the development of a provincial (Jiangsu) emission inventory, which can reduce the uncertainty in previous national level emission inventory and improve capability of air quality forecasting in Jiangsu province. The manuscript is well organized and written. Comprehensive evaluations were conducted, including comparisons with other inventories, with satellite data and with measurements of air pollutants. Another highlight of this manuscript is the inclusion of modeling results and sensitivity analysis of $PM_{2.5}$ and O_3 formation in Nanjing, which provides some implications of emission control strategies. The presentation of this newly developed high resolution emission inventory is suitable for being published in ACP.

Response and revisions:

We appreciate the reviewer's positive remarks on our manuscript.

2. Line 51-52: change “Issued in 2013, for example, the National Air Pollution Prevention Action Plan required” to “For example, the National Air Pollution Prevention Action Plan issued in 2013 required”.

Response and revisions:

We thank the reviewer’s suggestion and the sentence has been corrected as suggested **in lines 51-52 Page 3 in the revised manuscript.**

3. line 232: The sentence “For other sources, the temporal distributions in Shanghai investigated by Li et al. (2011).” is not complete.

Response and revisions:

We thank the reviewer’s reminder. The sentence has been revised as “For other sources, the temporal distributions for Shanghai investigated by Li et al. (2011) were adopted” **in lines 241-242 Page 10 in the revised manuscript.**

4. line 284-285: D3 also includes some areas of Anhui, Zhejiang and Shanghai, but the provincial inventory was developed for Jiangsu. How were emissions in D3 treated for provincial inventory case? Please clarify.

Response and revisions:

We thank the reviewer’s reminder and admit that we did not clarify the emission inventory applied in the provincial modeling case. In the provincial case, the emissions for the regions outside Jiangsu in D3 were obtained from the relocated 4×4 km regional inventory developed by Fu et al. (2013). Corresponding revision was shown **in lines 591-593 Page 22 in the revised manuscript.**

5. line 436-437: This implication might be questionable since the difference might be mainly driven by different methods (including different data sources) used in developments of emissions.

Response and revisions:

We thank the reviewer's comment and agree that the implication could not be sufficiently supported. The sentence has been removed in the revised manuscript.

6. Sect. 3.3 shows the comparisons of pollutants from typical sources, how about pollutants from all sources? As shown in Figure 3, these typical sources account for significant but not entire amounts of the selected pollutants. The spatial distributions of total pollutants may substantially differ.

Response and revisions:

We thank the reviewer's comment. The main purpose of Section 3.3 is not to compare the spatial distribution of the total emissions between inventories, but to investigate the influence of different methods and data sources on the spatial distribution of pollutants in emission estimation. Therefore emissions from selected sources are included in the comparisons between inventories at national and provincial scales. For example, industrial combustion was generally treated as area sources in the national inventory, while information of 6,194 point sources was collected and compiled in this work to develop the provincial inventory. The linear regression analysis between gridded emissions of industrial combustion in provincial and national inventories thus implies the deviations in spatial distributions of emissions resulting from different methods and data.

7. Page 19, line 514: NO_x emissions in Jiangsu are only 65% higher than those of Shanghai. Given the large areas of Jiangsu, NO_x emissions in south Jiangsu areas are

comparable to those in Shanghai, and south Jiangsu is very close to Shanghai. It is hard to say local source in south Jiangsu is dominant. Is “those of Shanghai and Zhejiang Shanghai” a typo? Please correct it.

Response and revisions:

We thank the reviewer's reminder and admit a mistake in the original sentence. Jiangsu's NO_x emissions were estimated 282% instead of 65% higher than Shanghai's in MEIC, and they were also 65% and 94% larger than those of another two contiguous provinces Zhejiang and Anhui, respectively. According to the YRD regional inventory by Fu et al. (2013), moreover, NO_x emissions of Suzhou and Wuxi in southern Jiangsu were nearly twice of those for the nearby cities Jiaxing and Huzhou in northern Zhejiang. Therefore we believe the local emissions played an important role in air pollution level in southern Jiangsu. **In lines 537-538 Page 20 in the revised manuscript**, the word "dominated" has been deleted and the sentence has been modified accordingly.

8. Sect. 4.2: Provincial emission inventory was developed but the innermost domain was only configured with focus on south Jiangsu. However, the newly developed emission in north Jiangsu might have impacts on the air quality simulations in south Jiangsu (as shown in Figure S6, some sources are from north). Besides, the evaluations using surface measurements were only shown in Nanjing, how about in other cities, particularly in north Jiangsu?

Response and revisions:

We thank the reviewer's comment. Compared to northern regions, intensive economy and industry are located in the more developed southern Jiangsu, thus the air quality issue is more concerned in the region. In this work, the emissions of SO₂, NO_x, CO, TSP, PM₁₀, PM_{2.5}, BC, OC, CO₂ and VOCs in the five cities in southern Jiangsu were estimated to contribute collectively 54.1%, 53.3%, 47.2%, 52.4%, 48.8%, 48.6%,

42.7%, 30.2%, 56.3% and 48.4% to the total emissions of the whole province in 2012, respectively. As shown in Figure S3, grids with relative large emissions (red color) were mainly clustered in southern Jiangsu. Therefore, we focused mainly on southern Jiangsu in the air quality simulation. As the emissions from northern Jiangsu were just applied in D2 simulation that provided the boundary conditions for D3 simulation, we believe the effects of those emissions were limited.

Regarding the model evaluation, the official data on air quality from surface measurements have been routinely published since 2013, thus the complete data for Jiangsu were unavailable for the years before 2013, except for its capital city Nanjing. Therefore only the observations at the nine sites in Nanjing were applied in this work.

9. *Page 23, line 641-642: How were VOCs mapped to VOCs species? Were the same species profile applied for three emission inventories? Please clarify.*

Response and revisions:

We thank the reviewer's comment. In this work, total NMVOC emissions for given source type in Table S1 were broken down into individual species using Eq. (1):

$$E(i,k) = E(i) \times X(i,k) \quad (1)$$

where E and X are the emissions and the chemical profile of VOCs (%), respectively; i and k represent the source type and individual VOCs species, respectively.

Different species profiles were applied in various inventories. The chemical profiles were mainly taken from domestic measurements, including residential fossil fuel and biomass burning, open biomass burning, on-road transportation, iron & steel, paint production, solvent use and oil refineries. For sources without sufficient local measurements, results from foreign studies were applied including the SPECIATE database by USEPA (2014). To reduce the possible uncertainty of source profile from individual measurement, Li et al. (2014) developed the "composite profiles" for sources where multiple candidate profiles were available, by revising the oxygenated

volatile organic compounds (OVOCs) fraction and averaging the fractions in different profiles for each species. In this work, “composite profiles” were updated following the method by Li et al. (2014), and the most recent source profiles from domestic results were contained.

To meet the requirement of CMAQ modeling, VOCs emissions were assigned to chemical mechanism (Carbon Bond 05) species by multiplying the emissions of individual species and mechanism-specific conversion factors:

$$E(i,m) = \frac{E(i,k)}{M(k)} \times C(k,m) \quad (2)$$

where E , M , and C are the emissions, mole weight, and the conversion factor, respectively; i , m , and k represent the source type, individual species, and the chemical mechanism species, respectively.

All the details could be found in another paper specifically for the development and evaluation of provincial VOC emission inventory (Zhao et al., in preparation), and we have stated that **in lines 232-234 Page 9, and in lines 681-683 Page 25 in the revised manuscript.**

10. *Figure S5: the wind vectors and colors are difficult to read, please make clearer plots.*

Response and revisions:

We thank the reviewer’s suggestion and an updated Figure S5 with clearer plots has been provided in the revised supplement.

11. *Page 26, line 716-721: Please clarify the starting time in Figure S6. Are surface winds plotted in figure S5? Wind directions vary at different heights (for example, blue red and green lines show different directions), so it cannot imply the inconsistency*

with WRF results. The trajectories include vertical information, but the WRF winds are horizontal winds.

Response and revisions:

We thank the reviewer's reminder. HYSPLIT 24 h back-trajectories at 50, 250 and 500 m are calculated every 6 hours starting at 11pm on 9th October and ending at 5 am on 8th October **(The caption of Figure S6 in the supplement has been revised)**. Figure S6 showed the air flow at the height of 50, 100 and 200m originated from Xuanwuhu site. Given the height of the first modeling layer in WRF was set at 50 m, the back trajectory at 50 m should be more suitable to indicate the air transport from 5 am on 8th to 11 pm on 9th October. As indicated in Figure S6 in the supplement, the air mass at 50 m altitude (the red line) came from northeast at 11pm on 9th October. However, the result was notably different with that simulated by WRF, in which the dominant wind direction was northwest (150°-170°) at that time.

Reviewer #2

1. This manuscript presents the development and evaluation of detailed emission inventories for major anthropogenic emission sources in Jiangsu Province, China. Emission is one of the major sources of uncertainty chemical transport modeling in China, where air pollution poses increasing threat to public health. Although it focuses only on one province (a relatively small emitter), which limits its scientific value to the broad ACP readership, this work could help establish procedures to develop and improve similar emission inventories in other provinces in this region. This manuscript could be improved in several key aspects to meet the requirements ACP. First, the presentation, in the current form, needs to be polished. There are several places in the text that the expression is either ambiguous or confusing. Second, the manuscript lacks detailed information on how these inventories were compiled (formula, parameters, etc), and where to find the key information to verify or reproduce the results reported here. Third, some of the materials included here are not

relevant to the main theme. For example, the sensitivity of ozone and PM_{2.5} to 50% reduction of NO_x and VOC emissions has nothing to do with development and evaluation of the emission inventories. The authors may consider either broadening the theme (development, evaluation, and application of the EIs) or removing the sensitivity section. Finally, the interpretation of some results need to be toned down or adjusted.

Response and revisions:

We appreciate the reviewer's crucial and important comments. In general, the presentation of the work has been improved, based on specific comments/suggestion from the reviewer. Detailed information on emission inventory development has been added, as indicated in the response to Questions 4, 7, 9, and 11 from the reviewer. In particular, Table S1 has been expanded and a new Table S3 has been added in the supplement to provide more detailed information on data sources of activities and emission factors. We also take the reviewer's suggestion and broaden the theme by adding the word "application" in the title of the paper. Uncertainties of the analysis have been also discussed to avoid overstatement of the work, as indicated in the response to Questions 14 and 16 from the reviewer.

2. L6: process(es).

Response and revisions:

We thank the reviewer's reminder and it is now corrected.

3. L26-30: *Please reword this sentence. Define "unfavorable meteorology". Is the meteorology simulated by WRF inaccurate or the meteorology condition not conducive to pollution formation and accumulation? If the meteorology simulation is problematic, emission may reduce the model bias by offsetting opposite bias caused by meteorology inputs, but that does not warrant the quality of emission data per se.*

Response and revisions:

The term “unfavorable meteorology” mentioned in the manuscript referred to the meteorology condition with low wind speed and PBL height, in which horizontal and vertical movement of atmosphere was limited. Under such condition, primary pollutants from large emitters would be easily accumulated over time, and air quality would thus be largely influenced by local sources. The sentence has been revised as “Under the unfavorable meteorology in which horizontal and vertical movement of atmosphere was limited, the simulated SO₂ concentrations at downtown Nanjing (the capital city of Jiangsu) using the regional or national inventories were much higher than observation, implying the overestimated urban emissions when economy or population densities were applied to downscale or allocate the emissions” **in lines 26-31 Pages 2-3 in the revised manuscript.**

We also agree with the reviewer that uncertainties existed in meteorology field simulation and that the performance of air quality modeling might be offset by the opposite bias of emission inventory and simulated meteorology. To test the deviation caused by meteorology field simulation with WRF, the model performance of SO₂ was reevaluated excluding the data from 5pm Oct 9th to 5am 10th. The normalized mean bias (NMB) were recalculated at -13%, 66%, and 50%, and the normalized mean errors (NME) were 45%, 88%, and 78% using the provincial, regional, and national inventories, respectively. This result thus implied that the provincial inventory could better support the air quality modeling, even uncertainties existed in meteorology field simulation.

4. *Section 2.1: There are at least eight sectors considered here. Is Eq. (1) applied to all sectors or only to point sources? In the case that other formulas are used, please explain in more details (only citations are briefly provided here). It will be very useful to provide a table that includes the following key information: 1) sector; 2) sources*

included in that sector; 3) method to estimate emission; 4) key parameters and data sources to obtain the information; 5) special adjustment made.

Response and revisions:

We thank the reviewer's important comment. We checked the sectors, and confirmed that there are seven main sectors (residential & commercial is one sector). We have stated **in line 133 Page 6 in the revised manuscript** that Eq. (1) is applied only to point sources. No equation is provided for mobile sources (i.e., on-road vehicles) as their emissions were estimated using COPERT model. We have also provided the equation and explanation for calculating the emissions from area sources **in lines 148-151 Page 7 in the revised manuscript**. As suggested by the reviewer, the detailed source categories by sector and the main data sources of activity levels by category were summarized **in the revised Table S1 in the supplement**. We keep the discussions on data sources of emission factors by category in Section 2.3, with the detailed information provided **in Table S2 and a new Table S3 in the supplement**, as explained in the response to Q7.

5. L177: which model requirement?

Response and revisions:

We thank the reviewer's reminder and admit the original word was confusing. The "model" here indicates COPERT 4 applied for calculating the emissions from on-road vehicles. Since differences exist in the categories of vehicle types between Chinese and European criteria, population of each Chinese vehicle category should be converted to the number consistent with the COPERT categories, in order to use the model. According to Cai and Xie (2007), for example, the buses, passenger cars (PC), heavy-duty trucks (HDT), light-duty trucks (LDT), and motorcycles (MT) in COPERT 4 indicate the big-size and middle-size passenger cars, small-size and mini passenger cars, heavy-duty and intermediate duty trucks, light-duty and mini trucks, and motorcycles in Chinese statistic system. The original sentence has been modified

as “Populations of different vehicle types were derived from statistical yearbooks by city and then converted to the numbers in COPERT 4 categories” **in lines 183-184 Page 8 in the revised manuscript.**

6. L181-185: Can not understand this sentence. Please rephrase it. It seems a subtraction is involved here, by using data from different sources. What is the implication for uncertainty by subtracting data from different sources?

Response and revisions:

We thank the reviewer’s important comment. In this work, as indicated in lines in the revised manuscript, information from the official environmental statistics, Pollution Source Census (PSC), and on-site survey on large emitters were collected to estimate the emissions from point sources. Although most of large industry sources could be investigated through this method, information of certain small plants were not included in those datasets and had to be treated as area sources. Thus the energy consumption and production provided in provincial statistical yearbooks were applied to check the completeness of point source investigation, and the difference between the energy statistics and overall activity levels of point sources was assumed as the activity levels of industrial area sources. The sentence has been revised as “For area sources, the coal consumption of residential activities was directly taken from National Energy Statistic Yearbook (NBSC, 2013c), while that of small industrial plants were calculated by subtracting the coal consumed by industrial point sources from the coal consumption of total industry provided in the provincial energy balance (NBSC, 2013c)” **in lines 188-192 Page 8 in the revised manuscript.**

7. Section 2.3. Again, a list of emission factors for each sector/source will be very useful. Maybe a table in the supplementary information.

Response and revisions:

We thank the reviewer's important comment. As required by the reviewer, a new Table S3 was provided **in the revised supplement**, summarizing the detailed emission factors and their sources by sector.

8. L227: *"by with"? Please revise the sentence.*

Response and revisions:

We thank the reviewer's reminder and admit the typo error. Now the error has been corrected **in line 237 Page 10 in the revised manuscript**.

9. L233-240. *Please provide information of the spatial maps used to distribute emissions for each sector. Currently only the data for open burning have been given.*

Response and revisions:

We thank the reviewer's suggestion and agree that more detailed information on spatial distribution of emissions should be provided. For point sources, information of latitude and longitude for each plant was collected from PSC. Locations of the total 6750 point sources shown in Figure S2 in the supplement were verified and modified in Google Earth. The road and hydrographic net in Jiangsu were respectively used to distribute the emissions from on-road transportation and ships city-by city.

Densities of GDP and population in Jiangsu applied to allocate emissions of area sources were from the research by Huang et al. (2014) and Fu et al. (2014). NH₃ emissions from livestock, fertilizer usage and agricultural vehicles were allocated by incorporating the population density and distribution of land types categorized to agricultural activities from the land cover dataset GlobCover2009 (<http://globalchange.nsd.cn>). Such information has been added **in lines 243-256 Page 10 in the revised manuscript**.

10. L280: *“initial (concentration) and boundary conditions”*

Response and revisions:

We thank the reviewer’s reminder and the text has been corrected **in line 293 Page 11 in the revised manuscript.**

11. L290-291: *Please elaborate how the vertical distribution is determined here. Is this applied to all sectors or just point sources?*

Response and revisions:

We thank the reviewer’s important suggestion and admit that it was not clearly explained in the original manuscripts. The vertical distributions of emissions were directly taken from L. Wang et al. (2010) except for the power sector, as the height of discharge outlet for each power plant was available for Jiangsu. According to L. Wang et al. (2010), the fractions of emissions of industry sources were 50%, 30% and 20% in layers 1-3, respectively. For the sources near the surface, i.e., transportation, residential & commercial combustion, solvent use, agriculture, and other sources, emissions were overall allocated to the first vertical layer in the model. The emissions of power plants were concentrated in layers 2-5, with the fractions estimated as 14.7%, 45.7%, 34.9% and 4.7%, respectively, based on the height information of the stacks. We have added the information **in lines 304-311 Page 12 in the revised manuscript.**

12. L447-449: *Is the agricultural GDP increase due to change in market price or commodity quantity?*

Response and revisions:

We thank the reviewer’s crucial comment and agree that application of commodity quantity would be more reasonable and persuasive to illustrate the case. We have checked the growth of livestock and poultry in Jiangsu from the provincial statistics.

In lines 465-468 Page 17 in the revised manuscript, the sentence has been modified as “According to the provincial statistics, the total numbers of livestock and poultry increased 6% and 10% from 2010 to 2012 in Jiangsu (JSNBS, 2013). The growth of activity levels was expected to result in enhanced emissions, as very little progress was achieved for NH₃ control for these years.”

13. Section 2 may need a sub-section to describe the measurement data (satellite and ground observations) used in this study.

Response and revisions:

We thank the reviewer’s comment. The ground observation and retrieval of satellite data were not the main tasks of this study, and the data were directly taken from other publication/groups without any extra modification. Therefore, we do not think it is necessary to describe the data in a specific section, and we have kept the description in corresponding sections in the revised manuscript, i.e., **lines 593-599** for ground observations and **lines 526-534 Pages 19-20** for satellite observation.

14. Section 4.1 Using satellite NO₂ data for emission evaluation has been well explored (check the literature for more details). There are several issues related to the method used here. Note OMI observes VCD, not emission. Therefore, it may make more sense to compare the VCD from OMI to the equivalent from CMAQ, not the emission distribution directly, unless the nonlinear relationship between emission and VCD is accounted for. In addition, the noise to signal ratio in OMI NO₂ increases with decreasing VCD. The interpretation of the correlation between emission and OMI VCD needs to consider these factors.

Response and revisions:

We thank the reviewer’s very important comment and agree that the uncertainty of the method should be discussed in the paper. First, the quality control and

reliability of OMI retrieved NO₂ VCDs has been added in **lines 529-534 Pages 19-20 in the revised manuscript** with literature provided. We then acknowledged that the comparisons between spatial distribution of NO₂ VCDs and emissions should be cautiously interpreted particularly for regions with relatively low values, as the noise to signal ratio in OMI NO₂ increases with decreased VCDs. Although summer NO₂ VCDs were applied in this study to eliminate the effects of long lifetime of NO₂ on pollution plums transport and chemical reaction, non-linear relationship still exists between VCDs and emissions. More detailed comparisons between NO₂ from satellite observation and CTM are thus recommended when improved characterization of NO₂ vertical distribution is available for the region. We have added such discussions **in lines 576-582 Page 21 in the revised manuscript**.

15. Section 4.3: It is good to see that the new emission inventories can reduce high bias during extreme events when the meteorology is not correctly simulated. Do we have any results showing that this emission data can be used to improve prediction of real pollution events? This manuscript discusses the new emission data for the entire province. Why is only the model prediction over Nanjing discussed in the model-observation comparison?

Response and revisions:

We thank the reviewer's positive remarks and suggestion. As shown in Table 2, better model performances for SO₂, NO_x, O₃ and PM_{2.5} simulation could be achieved with provincial inventory than those with national or regional inventory for the whole October, implying the improvement of provincial emission inventory for Jiangsu. Besides the special case discussed in Section 4.3, the simulated PM_{2.5} concentrations from 8pm on 18th to 5pm on 19th October with different inventories could also indicate the advantage of the provincial inventory against the regional and national inventories in a pollution event prediction. Taking Caochangmen (CCM) site as the example, the observed PM_{2.5} concentration kept increasing from 8pm on 18th with the highest value reaching 114 µg/m³ at 2am on 19th. Simulated PM_{2.5} concentrations with

provincial, regional and national inventory at that time were 90, 53 and 45 $\mu\text{g}/\text{m}^3$, respectively. The correlation coefficients between observations and simulations with the three inventories were calculated as 0.66, 0.44 and 0.30 in the episode, respectively, indicating the better performance with provincial inventory in real pollution episode simulation. We have added such discussions **in lines 619-626 Page 23 in the revised manuscript.**

Regarding the second question, the official data on air quality from surface measurements have been routinely published since 2013, thus the complete data for Jiangsu were unavailable for the years before 2013, except for its capital city Nanjing. Therefore only the observations at the nine sites in Nanjing were applied in this work.

16. As mentioned earlier, this section may not be necessary to support the main argument here. The interpretation of the results needs to acknowledge several caveats in the design and scope of these simulations. For instance, the brute force method does not consider nonlinearity in ozone response to precursor change. Large uncertainties exist in the emission dataset, including VOCs that have not been evaluated here, which will affect the chemistry and directionality of the ozone response. In addition, the sensitivity examines ozone response, but NO_x and VOCs changes also result in changes in other pollutants, such as PM_{2.5}. It is hence premature to draw such conclusion as in L770-772.

Response and revisions:

We thank the reviewer's very crucial comment and suggestion. As suggested, we revised the title of the paper, stressing the "application" of the emission inventory. We agree with the reviewer that the brute-force method ignores the nonlinearity of O₃ response to the changes of precursor emissions, and that is a big uncertainty of the analysis. The results should thus be cautiously interpreted, and the comparisons with other simulation methods that take the nonlinearity mechanisms into account (e.g.,

OSAT or tagged species method) are further recommended. We have added the discussions **in lines 825-831 Page 30 in the revised manuscript.**

For VOC, the detailed information on development and evaluation of provincial inventory with source profiles is presented in a separate paper (Zhao et al., in preparation). Regarding the length of current paper, we have briefly stated that in **lines 232-234 Page 9, and in lines 681-683 Page 25 in the revised manuscript.**

We also agree with the reviewer that the air quality includes many issues besides O₃ problem, thus the sentence in lines 770-772 in the original manuscript has been deleted to avoid overstating the case.

References

- Boersma, K. F., Eskes, H. J., Dirksen, R. J., van der A, R. J., Veefkind, J. P., Stammes, P., Huijnen, V., Kleipool, Q. L., Sneep, M., Claas, J., Leitão, J., Richter, A., Zhou, Y., and Brunner, D.: An improved tropospheric NO₂ column retrieval algorithm for the Ozone Monitoring Instrument, *Atmos. Meas. Tech.*, 4, 1905–1928, doi: 10.5194/amt-4-1905-2011, 2011.
- Cai, H., Xie, S. D.: Estimation of vehicular emission inventories in China from 1980 to 2005, *Atmos. Environ.*, 41, 8963-8979, 2007.
- Fu, J. Y., Jiang, D., Huang, Y. H.: 1 Km Grid Population Dataset of China (PopulationGrid_China), Global Change Research Data Publishing & Repository, DOI: 10.3974/geodb.2014.01.06. V1, 2014.
- Fu, X., Wang, S. X., Zhao, B., Xing, J., Cheng, Z., Liu, H., and Hao, J. M.: Emission inventory of primary pollutants and chemical speciation in 2010 for the Yangtze River Delta region, China, *Atmos. Environ.*, 70, 39-50, 2013.
- Han, K. M., Lee, S., Chang, L. S., Song, C. H.: A comparison study between CMAQ-simulated and OMI-retrieved NO₂ columns over East Asia for evaluation of NO_x emission fluxes of INTEx-B, CAPSS, and REAS inventories. *Atmos. Chem. Phys.*, 15, 1913-1938, 2015.
- Huang, K., Fu, J. S., Gao, Y., Dong, X. Y., Zhuang, G. S., Lin, Y. F.: Role of sectoral and multi-pollutant emission control strategies in improving atmospheric visibility in the Yangtze River Delta, China. *Environ. Pollution*, 184: 426-434, 2014.
- Huang, Y. H., Jiang, D., Fu, J. Y.: 1 Km Grid GDP Data of China (2005, 2010) (GDPGrid_China), Global Change Research Data Publishing & Repository, DOI:

10.3974/geodb.2014.01.07. V1, 2014.

JSNBS (Jiangsu Bureau of Statistics): Statistical Yearbook of Jiangsu, Beijing, China Statistics Press, 2013 (in Chinese).

Li, L., Chen, C. H., Fu, J. S., Huang, C., Streets, D. G., Huang, Y. H., Zhuang, G. F., Wang, J. Y., Jang, C. J., Wang, H. L., Chen, Y. R., and Fu, M. J.: Air quality and emissions in the Yangtze River Delta, China, *Atmos. Chem. Phys.*, 11, 1621-1639, doi:10.5194/acp-11-1621-2011, 2011.

Li, M., Zhang, Q., Streets, D. G., He, K. B., Cheng, Y. F., Emmons, L. K., Huo, H., Kang, S. C., Lu, Z., Shao, M., Su, H., Yu, X., and Zhang, Y.: Mapping Asian anthropogenic emissions of non-methane volatile organic compounds to multiple chemical mechanisms, *Atmos. Chem. Phys.*, 14, 5617-5638, 2014.

U.S. Environmental Protection Agency (USEPA): SPECIATE Version 4.4, available at: <https://www3.epa.gov/ttnchie1/software/speciate> (last access: 12 November 2015), 2014.

Wang, L. T., Jang, C., Zhang, Y., Wang, K., Zhang, Q., Streets, D. G., Fu, C. J., Lei, Y., Schreifels, J., He, K. B., Hao, J. M., Lam, Y. F., Lin, J., Meskhidze, N., Voorhees S., Evarts D., Phillips S.: Assessment of air quality benefits from national air pollution control policies in China. Part II: Evaluation of air quality predictions and air quality benefits assessment. *Atmos. Environ.*, 44, 3449-3457, 2010.

Xia, Y. M., Zhao, Y., Nielsen, C. P.: The benefits of China's efforts in gaseous pollutant control indicated by the bottom-up emissions and satellite observations, *Atmos. Environ.*, 136, 43-53, 2016.

Zhao, Y., Mao, P., Zhou, Y., Yang, Y., Zhang, J., Wang, S., Dong, Y., Xie, F., Yu, Y., and Li, W.: Improved provincial emission inventory and speciation profiles of anthropogenic non-methane volatile organic compounds: a case study for Jiangsu, China, in preparation.

TITLE PAGE

Development of a high-resolution emission inventory and its evaluation and application through air quality modeling for Jiangsu Province, China

Yaduan Zhou¹, Yu Zhao^{1,2*}, Pan Mao¹, Qiang Zhang³, Jie Zhang^{2,4}, Liping Qiu¹, Yang Yang¹

1. State Key Laboratory of Pollution Control & Resource Reuse and School of the Environment, Nanjing University, 163 Xianlin Ave., Nanjing, Jiangsu 210023, China

2. Jiangsu Collaborative Innovation Center of Atmospheric Environment and Equipment Technology (CICAEET), Nanjing University of Information Science & Technology, Jiangsu 210044, China

3. Ministry of Education Key Laboratory for Earth System Modeling, Center for Earth System Science, Tsinghua University, Beijing 100084, China

4. Jiangsu Provincial Academy of Environmental Science, 176 North Jiangdong Rd., Nanjing, Jiangsu 210036, China

*Corresponding author: Yu Zhao

Phone: 86-25-89680650; email: yuzhao@nju.edu.cn

ABSTRACT

Improved emission inventories combining detailed source information are crucial for better understanding the atmospheric chemistry and effectively making emission control policies using air quality simulation, particularly at regional or local scales. With the downscaled inventories directly applied, chemical transport model might not be able to reproduce the authentic evolution of atmospheric pollution processes at small spatial scales. Using the bottom-up approach, a high-resolution emission inventory was developed for Jiangsu China, including SO₂, NO_x, CO, NH₃, volatile organic compounds (VOCs), total suspended particulates (TSP), PM₁₀, PM_{2.5}, black carbon (BC), organic carbon (OC), and CO₂. The key parameters relevant to emission estimation for over 6000 industrial sources were investigated, compiled and revised at plant level based on various data sources and on-site survey. As a result, the emission fractions of point sources were significantly elevated for most species. The improvement of this provincial inventory was evaluated through comparisons with other inventories at larger spatial scales, using satellite observation and air quality modeling. Compared to the downscaled Multi-resolution Emission Inventory for China (MEIC), the spatial distribution of NO_x emissions in our provincial inventory was more consistent with summer tropospheric NO₂ VCDs observed from OMI, particularly for the grids with moderate emission levels, implying the improved emission estimation for small and medium industrial plants by this work. Three inventories (national, regional, and provincial by this work) were applied in the Models-3/Community Multi-scale Air Quality (CMAQ) system for southern Jiangsu October 2012, to evaluate the model performances with different emission inputs. The best agreement between available ground observation and simulation was found when the provincial inventory was applied, indicated by the smallest normalized mean bias (NMB) and normalized mean errors (NME) for all the concerned species SO₂, NO₂, O₃ and PM_{2.5}. The result thus implied the advantage of improved emission inventory at local scale for high resolution air quality modeling. Under the unfavorable meteorology, in which horizontal and vertical movement of atmosphere was limited, the simulated SO₂ concentrations at downtown Nanjing (the capital city of Jiangsu) using the regional or national inventories were much higher than observation, implying the

删除的内容: for

删除的内容: pollution transport, in particular

删除的内容: much higher

删除的内容:

删除的内容: were simulated for downtown Nanjing (the capital city of Jiangsu) using the regional or national inventories

30 | ~~overestimated urban emissions when economy or population densities were applied to~~
31 downscale or allocate the emissions. With more accurate spatial distribution of emissions at
32 city level, the simulated concentrations using the provincial inventory were much closer to
33 observation. Sensitivity analysis of PM_{2.5} and O₃ formation was conducted using the
34 improved provincial inventory through the Brute Force method. Iron & steel and cement
35 plants were identified as important contributors to the PM_{2.5} concentrations in Nanjing. The
36 O₃ formation was VOCs-limited in southern Jiangsu, and the concentrations were negatively
37 correlated with NO_x emissions in urban areas owing to the accumulated NO_x from
38 transportation. More evaluations are further suggested for the impacts of speciation and
39 temporal and vertical distribution of emissions on air quality modeling at regional or local
40 scales in China.

删除的内容: overestimation

删除的内容: in

删除的内容: the locations of
large emitters were not fully
considered, and the densities of

删除的内容: simply

42 1 INTRODUCTION

43 With rapid development of economy and growth of energy consumption, eastern China is
44 experiencing severe atmospheric pollution attributed to the large emissions of primary air
45 pollutants and the subsequent formation of secondary pollution, e.g., fine particles and O₃.
46 Relatively high concentrations of surface PM_{2.5} were observed in eastern China based on the
47 national monitoring network (data source: <http://106.37.208.233/>), and only 9.5% out of 190
48 cities with the measurement data reported in 2014 met the National Ambient Air Quality
49 Standard (NAAQS), i.e., 35 µg/m³ for annual PM_{2.5} concentration (MEP, 2012). Under the
50 serious case of air pollution, series of measures have been conducted to reduce the pollutant
51 emissions and to improve the air quality across the country. For example, the National Air
52 Pollution Prevention Action Plan issued in 2013 required strict emission controls on both
53 industry and transportation sectors, and aimed to achieve a 25%, 20% and 15% reduction of
54 annual PM_{2.5} concentration for Beijing-Tianjin-Hebei (JJJ), Yangtze River Delta (YRD), and
55 Pearl River Delta (PRD) region from 2012 to 2017, respectively. Given the non-linear
56 response of ambient concentrations to emissions, chemical transport modeling (CTM) has
57 been widely applied to study the mechanisms of complex pollution processes and the impacts
58 of emission abatement (Zhang et al., 2006; Streets et al., 2007; B. Zhao et al., 2013; Zhang et

59 al., 2012). As the key input of CTM, therefore, improved emission inventories, particularly at
60 regional or local scales, become important for scientific air quality simulation and effective
61 policy making.

62 Progress has been increasingly achieved in emission inventory studies for China.
63 Compared to earlier national emission inventories including those for Transport and Chemical
64 Evolution over the Pacific Mission (TRACE-P, Streets et al., 2003), Intercontinental Chemical
65 Transport Experiment-Phase B (INTEX-B, Zhang et al., 2009), and Regional Emission
66 inventory in Asia (REAS, Ohara et al., 2007; Kurokawa et al., 2013), Tsinghua University
67 developed the Multi-resolution Emission Inventory for China (MEIC,
68 <http://www.meicmodel.org/>), in which the information of large power plants and cement
69 factories was investigated and the uncertainties of emission estimation for those typical
70 sources were reduced (Wang et al., 2014). Besides, high-resolution emission inventories at
71 regional and city scales were gradually established in the developed regions JJJ, YRD and
72 PRD, attributed to better data support and stronger need to combat air pollution (Zheng et al.,
73 2009; S. Wang et al., 2010; Huang et al., 2011; B. Zhao et al., 2012; Zhao et al., 2015).

74 Resulting from various methods and data sources, clear discrepancies exist in different
75 emission inventories in China, both at national (Y. Zhao et al., 2013; Xia et al., 2016) and
76 local scales (Zhao et al., 2015). When applied in CTM, the uncertainties in emission
77 estimation would inevitably lead to bias in air quality simulation, besides the errors of
78 meteorological field modeling and deficiencies of built-in atmospheric chemical mechanisms
79 (Zheng et al., 2012). Based on the Models-3/Community Multi-scale Air Quality (CMAQ)
80 system, for example, Zhang et al. (2014) simulated $PM_{2.5}$ and O_3 concentrations in
81 southeastern United States using the different versions of national emission inventory (NEI),
82 and compared the results with several ground observational datasets. The model performance
83 with updated inventory (NEI05) was much better than that with old one (NEI99), indicating
84 the impacts of emission inventory on the accuracy of CMAQ simulations. Han et al. (2015)
85 conducted NO_2 vertical column simulation for China with CMAQ, and found that the
86 modeled results using INTEX-B inventory were closer to satellite observation than those
87 using REAS. At regional or local scales, emission inventory that incorporates the detailed
88 information of individual sources is assumed to have advantages in air quality research prior

to downscaled national inventory that generally applied regional average levels of emission factors due to unavailability of data (Zhao et al., 2015). The benefits of improved emission estimation, spatial and temporal distribution, or chemical speciation of pollutants, however, have not been sufficiently confirmed with CTM. Recently, Yin et al. (2015) conducted CMAQ simulation on O₃ using updated VOC emission inventory for PRD, implying that the reduced uncertainties of total emission estimation and spatial distribution could improve the model performance compared with ground observation.

We select Jiangsu, a typical province with well-developed industry in eastern China, to develop and evaluate the high-resolution emission inventory. The geographic location and cities of the province are illustrated in Figure S1 in the supplement. With a total area of 107 200 km² and population of 79.2 million in 2012, Jiangsu was the first ranked province in gross domestic product (GDP) per capita in China (NBSC, 2013a; JSNBS, 2013). It accounted for 8.0%, 7.6%, 8.9%, and 10.2% of the country's power generation, cement, pig iron, and crude steel production in 2012, respectively (NBSC, 2013b). Intensive energy consumption and industry resulted in heavy air pollution: all the 13 cities had their annual average concentrations of PM_{2.5} exceeding the NAAQS in 2012, with the highest reaching 74 µg/m³ in the capital city, Nanjing. Clear uncertainties exist in current multi-scale emission inventories. Zhao et al. (2015), for example, estimated Nanjing's SO₂ and PM_{2.5} emissions at 165 and 71 Gg in 2012, respectively, while the results by Fu et al. (2013) were 131.8 and 35.3 Gg, implying the necessity of improvement and assessment of regional emission inventory, for both scientific and policy implication. In this work, a comprehensive emission inventory for Jiangsu with high temporal and spatial resolutions was first established with the best available data of local emission sources incorporated. This provincial emission inventory was then compared with other inventories and satellite observation to test its improvement on emission estimation and spatial distribution. CMAQ was further applied to indicate the advantage of the provincial inventory prior to downscaled national and regional ones. In particular, the impacts of spatial distribution of emissions on model performance were analyzed for period with unfavorable meteorological condition. Finally, the improved inventory was applied for sensitivity analysis on regional PM_{2.5} and O₃ formation.

2 DATA AND METHODS

2.1 Methodology of provincial emission inventory development

The emissions of gaseous pollutants (SO₂, NO_x, CO, NH₃ and VOCs), greenhouse gas CO₂, particulate matter (total suspended particulates, TSP, PM₁₀ and PM_{2.5}) and its chemical compositions (black carbon, BC and organic carbon, OC) of anthropogenic origin in Jiangsu were estimated with a bottom-up method. Emission sources were classified into seven main categories, including power plant, industry, solvent use, transportation, residential & commercial, agriculture and other sources. Industry was subdivided into iron & steel, cement, and other industry including nonferrous metal smelting, brick and lime kilns, chemical industry and other industry boilers. Residential & commercial sector included household combustion of fossil fuel and biofuel. Agriculture included livestock and fertilizer usage. Open biomass burning, cooking, and waste (water) disposal, were considered as other sources. The detailed categories were summarized in Table S1 in the supplement. For each category, point, mobile and area sources were defined depending on the detailed levels of information and the emission characteristics. For point sources, information on emission factor and activity level was investigated and compiled for individual plants, and the annual emissions of atmospheric pollutants were calculated using Eq. (1), as described in Zhao et al (2015).

$$E_i = \sum_{j,m} AL_{i,j,m} \times EF_{i,j,m} \times (1 - \eta_{i,j,m}) \quad (1)$$

where i, j and m represented the pollutant species, individual plant, and fuel/technology type, respectively; AL was the activity level data; EF was the uncontrolled emission factor; and η was removal efficiency of air pollutant control device.

Regarded as mobile sources, the emissions of on-road transportation were calculated by the CORPERT model (EEA, 2012) and then spatially allocated based on the road net information of the province. Area sources included non-road transportation, solvent use, residential & commercial sector, agriculture, and small industry plants without detailed information collected. The emissions from non-road transportation and agriculture were estimated following the methods by Zhang et al. (2010) and Dong et al. (2009), respectively.

For other sources, the emissions were calculated using Eq. (2)

$$E_{i,n} = \sum_m AL_{i,m,n} \times EF_{i,m,n} \times (1 - \eta_{i,m,n}) \quad (2)$$

where n represented the source type; EF_n and η_n were the average levels of uncontrolled emission factors and removal efficiencies for given source n . For sources without any emission control measure (e.g., residential combustion), $\eta=0$.

2.2 Activity level

The main sources of activity data are summarized by category in Table S1 in the supplement. Most of coals in Jiangsu were used by power and industry sectors, and household accounted for only 0.3% of total coal consumption in the province in 2012 (JSNBS, 2013), indicating the significance to reduce the uncertainties of emission estimation for power and industry plants. Therefore a comprehensive database for power and industrial sector was established with the information collected and modified from the official environmental statistics, Pollution Source Census (PSC, internal data), and on-site survey on large emitters. Parameters including geographical location, combustion/production technology, fuel/burner/boiler type, installed air pollution control device (APCD) and its removal efficiency were investigated for individual plants. Totally 6750 plants were identified as point sources, including 191 power plants, 185 iron & steel plants, 231 cement factories, 707 lime and brick factories, 365 chemical plants and 5071 other industrial factories, as illustrated in Figure S2 in the supplement. In particular, the kilns for combustion and factories for calcination were separately investigated for cement production, and 25% of cement plants contained the both processes. For power, cement, and iron & steel sectors, the aggregated activity levels compiled plant by plant, i.e., the coal consumption of power generation, and the production of cement, clinker, coke, pig iron, and crude steel, were estimated at 108%, 95%, 120%, 109%, 104%, and 98% of the provincial statistics, respectively (JSNBS, 2013). The comparison indicates, on one hand, that larger activity levels would be obtained based on detailed investigation of individual emission sources than official statistics for power and most processes of iron & steel sectors. On the other hand, almost complete investigation on point sources was conducted for those sectors, as very small fractions of activities (5% for cement and 2% for steel production) had to be estimated as area sources. For other industrial

带格式的：非突出显示

带格式的：字体：倾斜

带格式的：字体：倾斜，下标

带格式的：字体：倾斜

带格式的：下标

带格式的：字体：倾斜

带格式的：字体：非倾斜

带格式的：缩进：首行缩进：0 字符

176 sectors, smaller fractions of point sources were achieved, e.g., 32% and 36% for ammonia and
177 sulfuric acid production, respectively.

178 For on-road transportation, the input parameters of COPERT 4 include regional
179 meteorological information, vehicle population by type, fleet composition by control stage
180 (China I–IV, equivalent to Euro I–IV), average vehicle speeds, and annual average kilometers
181 traveled (VKT). Monthly mean temperature and relative humidity were obtained from the
182 China Meteorological Data Sharing Service System (<http://www.escience.gov.cn>).

183 Populations of different vehicle types were derived from statistical yearbooks by city and then
184 converted to the numbers in COPERT 4 categories. The fleet composition by control stage
185 was obtained from the survey by local government (internal data, Zhao et al., 2015). Vehicle
186 speed by road type (i.e., freeway, arterial and residential road) and VKT by vehicle type were
187 determined according to previous studies (Cai and Xie, 2007; Wang et al., 2008) and the
188 guidebook of emission inventory development for Chinese cities (He, 2015). For area sources,
189 the coal consumption of residential activities was directly taken from National Energy
190 Statistic Yearbook (NBSC, 2013c), while that of small industrial plants were calculated by
191 subtracting the coal consumed by industrial point sources from the coal consumption of total
192 industry provided in the provincial energy balance (NBSC, 2013c). The original data on the
193 activity levels of agriculture, solvent use, non-road transportation and open biomass burning
194 were obtained from the provincial or city statistical yearbooks (JSBNS, 2013).

删除的内容: as

删除的内容: the

删除的内容: from

删除的内容: minus the coal
consumption of industrial point
sources

195 **2.3 Emission factor**

196 Following previous studies (Zhao et al., 2008; 2010; 2011; 2012a; 2012b; Y. Zhao et al.,
197 2013), an emission factor database for Jiangsu was established with detailed information and
198 available results of emission measurements on local sources incorporated. For power sector,
199 parameters relevant to emission factors were obtained at individual plant level including
200 installed capacity, fuel type and quality (e.g., sulfur and ash content), combustion technology,
201 and the type and removal efficiencies of APCDs. In particular, the information of APCD
202 installation obtained from provincial environmental statistics and on-site survey was further
203 corrected according to the official documents on APCD projects of power plants published by
204 Ministry of Environment Protection of China

(http://www.zhb.gov.cn/gkml/hbb/bgg/201305/t20130506_251654.htm). As summarized in Table S2 in the supplement, the application rates of flue gas desulfurization (FGD), selective catalytic reduction (SCR)/selective non-catalytic reduction (SNCR), and dust collectors for Jiangsu's power plants in 2012 were 97%, 57% and 99% in terms of coal consumption, and the average removal efficiencies of SO₂, NO_x and TSP weighted by coal consumption were calculated at 83.3%, 37.1% and 98.0%, respectively. Combining all the above-mentioned information, the emission factors for individual plant and facility were calculated using the methods developed by Zhao et al. (2010).

Table S3 in the supplement summarizes the emission factors of main industrial processes.

For iron & steel production, emission factors of the four main manufacturing processes (coking, sintering, pig iron production, and steel making) were estimated combining the unabated emission factors from previous database (Zhao et al., 2011; Y. Zhao et al., 2013) and the investigated information on penetrations and removal efficiencies of APCDs at plant level. Provided in Table S2, 64.3% of Jiangsu's iron & steel plants installed FGD in 2012 and the average SO₂ removal efficiency was estimated at 78.0%. Dust collectors were installed at almost all the furnaces for pig iron production and steel making, with the averages of PM removal efficiency estimated at 96% and 94%, respectively. For cement production, emission factors were calculated for the two main processes, coal combustion and calcination, following Lei et al. (2011). With dust collectors installed at 99% of plants, the average of overall removal efficiency on TSP was estimated at 97.3% according to our plant-by-plant investigation (Table S2).

For area sources, emission factors for non-road transportation were obtained from Zhang et al. (2010), Ye et al. (2014) and Fu et al. (2012). Emission factors for household fossil fuel and biofuel combustion were from the summary of field measurements in Y. Zhao et al. (2013). For agricultural activities including livestock and fertilizer use, emission factors were obtained from Dong et al. (2009) and Yin et al. (2010). Emission factors of VOCs were mainly from Wei et al. (2009) with update for typical sources based on limited local measurements and survey (Bo et al., 2008; EEA, 2013; Xia et al., 2014). The source profiles of VOC for Jiangsu were obtained following Li et al. (2014) with the most recent data from domestic results incorporated (Zhao et al., in preparation).

2.4 Temporal and spatial distributions

The monthly variations of emissions from power plants and industrial sources were assumed to be dominated by the variations of electricity generation and typical industrial production, respectively, and those data were obtained from National Bureau of Statistics of China (<http://data.stats.gov.cn/>). As the real-time monitoring on urban traffic was unavailable for the whole province, the temporal distribution of emissions from on-road vehicles in other cities was considered to be the same as Nanjing (Zhao et al., 2015). For other sources, the temporal distributions for Shanghai investigated by Li et al. (2011) were adopted.

Different parameters were used to conduct the spatial allocation of emissions by sector. Latitude and longitude of each point source collected from PSC were checked and revised according to Google Earth to avoid the unexpected errors in the existing database (Figure S2 in the supplement). The products of GDP (Huang et al., 2014) and population distribution with high resolution at 1km (Fu et al., 2014) were applied to allocate the emissions from industrial area sources and residential & commercial sources, respectively. Emissions from on-road transportation were allocated based on the road net by city. As the ship flow was unavailable, the widths of Yangtze River and the Grand Canal within Jiangsu were used as indicators for ship emissions. Emissions from open biomass burning were allocated by the locations and brightness of agricultural fire spots observed by MODIS (Moderate Resolution Imaging Spectroradiometer, <https://earthdata.nasa.gov/data/near-real-time-data/firms>). NH₃ emissions from livestock and fertilizer usage were allocated based on the density of rural population and the distribution of agricultural lands obtained from the land utilization dataset GlobCover_2009 (<http://globalchange.nsd.cn>).

2.5 Configuration of air quality modeling

The Models-3/Community Multi-scale Air Quality (CMAQ) version 4.7.1 was applied to evaluate the emission inventory for Jiangsu. As shown in Figure 1, three one-way nested domain modeling was conducted, and the spatial resolutions were set at 27, 9 and 3 km respectively in Lambert Conformal Conic projection, centered at (110° E, 34° N) with two true latitudes 25°N and 40°N. The mother domain (D1, 180×130 cells) covered most part of China, Japan and the whole Korea and part of other country. Jiangsu, Zhejiang, Shanghai,

删除的内容:

删除的内容: with

删除的内容: densities of

删除的内容: (J. Fu et al., 2014)

删除的内容: ,

删除的内容: and

删除的内容: by

删除的内容: with

删除的内容: land utilization
classification

264 Anhui and parts of other provinces were at the second modeling region (D2, 118×97 cells).
265 The third (D3, 124×70 cells) covered the mega city Shanghai and six most developed cities
266 in southern Jiangsu including Nanjing, Changzhou, Zhenjiang, Wuxi, Suzhou and Nantong.
267 The simulation period was selected from October 1 to 31, 2012, with the first five days
268 chosen as spin-up period to provide initial conditions for later simulations.

269 Meteorological fields were provided by the Weather Research and Forecasting Model
270 (WRF) version 3.4 with the main physical options set as Fu et al. (2013), and the outputs were
271 transferred by meteorology chemistry interface professor (MCIP) version 4.2 into the
272 chemistry transport module in CMAQ (CCTM). In WRF, the U.S. Geological Survey (USGS)
273 database was adapted as terrain and land use data, and the first guess field of meteorological
274 modeling was provided by the final analysis dataset (ds083.2) from National Centers for
275 Environmental Prediction (NCEP). Statistical indicators including Bias, Index of Agreement
276 (IOA), and root mean squared error (RMSE) were applied to evaluate the performance of
277 WRF modeling against observation (Baker, 2004; Zhang et al., 2006). Ground observations in
278 three hours interval at meteorological stations were downloaded from National Climatic Data
279 Center (NCDC), including 43 stations in the second modeling domain D2 and 7 stations in the
280 innermost domain D3 (as labeled in Figure 1). The statistics of those indicators for wind
281 speed and direction at 10 m (WS10 and WD10), temperature at 2 m (T2) and relative
282 humidity at 2 m (RH2) for October 2012 in D2 and D3 were summarized in Table [S4](#).
283 Discrepancies between WRF simulations and ground observations were within acceptable
284 range (Emory et al., 2001) and comparable to the results of other studies (Wang et al., 2014).
285 Better agreements were found for simulations of T2 and RH2 than WS10 and WD10. In spite
286 of moderate overestimation by 0.3% and 3.5% in T2 and RH2, the IOA of those two variables
287 were 0.97 and 0.90, indicating the high consistency with observational. Slightly higher than
288 observation in D2 and D3, simulated WS10 might enhance the diffusion process of pollutants
289 in atmosphere eventually and thus lead to underestimation in pollutant concentrations. For
290 WD10, the bias between simulations and observations was 3.6 degree in D3 within the
291 benchmark range (Emory et al., 2001).

292 The carbon bond gas-phase mechanism (CB05) and AERO5 aerosol module were
293 adopted in all the CMAQ modules. The initial [concentrations](#) and boundary conditions for

first modeling domain was the default clean profile, while for nested domain they were extracted from the CCTM outputs of its mother domain. Anthropogenic emissions used for domains D1 and D2 were obtained from the downscaled MEIC with an original spatial resolution of $0.25^{\circ} \times 0.25^{\circ}$. For Jiangsu domain in D3, three inventories, i.e., downscaled MEIC, the regional inventory of YRD by Fu et al. (2013), and the provincial inventory developed in this work, were used to test the modeling performance and potential improvement in emission estimation. In addition, biogenic emission inventory was from the Model Emissions of Gases and Aerosols from Nature developed under the Monitoring Atmospheric Composition and Climate project (MEGAN-MACC, Sindelarova et al., 2014), and the emission inventories of Cl, HCl and lightning NO_x were from the Global Emissions Initiative (GEIA, Price et al., 1997). The vertical distributions of emissions were directly taken from L. Wang et al. (2010) except for the power sector, as the height of discharge outlet for each plant was available. According to L. Wang et al. (2010), the fractions of emissions of industry sources were 50%, 30% and 20% in layers 1-3, respectively. For the sources near the surface, i.e., transportation, residential & commercial combustion, solvent use, agriculture, and other, emissions were overall allocated to the first vertical layer in the model. The emissions of power plants were concentrated in layers 2-5 with the fractions estimated at 14%, 46%, 35% and 5%, respectively, based on the height information of the stacks.

删除的内容: The vertical distribution of emissions was determined by source following L. Wang et al. (2010).

3 RESULTS

3.1 Emission estimation and sector contribution

The total annual emissions of SO_2 , NO_x , CO, TSP, PM_{10} , $\text{PM}_{2.5}$, BC, OC, CO_2 , NH_3 and VOCs were calculated at 1142, 1642, 7680, 2606, 1394, 941, 57, 138, 860458, 1100 and 1747 Gg for Jiangsu in 2012, respectively. The emissions by city were provided in Table 1. In general, higher emissions were found in cities in southern Jiangsu with large population and intensive economy and industry than those in northern Jiangsu. Taking 52% of the provincial industrial GDP, Suzhou, Nanjing, and Wuxi were estimated to collectively account for 41%, 41%, 35%, 31%, 43% and 39% of the total emissions of SO_2 , NO_x , CO, $\text{PM}_{2.5}$, CO_2 and VOCs, respectively. Xuzhou, different with other cities in northern Jiangsu, had a relative

high emissions of pollutants due to its well development of large-scale industry. Because of the active agricultural development, NH₃ emissions in Huai'an and Nantong were estimated at 195.9 and 187.1 Gg, significantly higher than other cities.

Shown in Figure 2 is the detailed sector contribution of pollutants from point, mobile (on-road transportation) and area sources. The point sources including power and industrial plants contributed 84%, 71%, 55%, 83%, 75%, 64%, 41%, 31%, 83%, 2% and 36%, to the total emissions of SO₂, NO_x, CO, TSP, PM₁₀, PM_{2.5}, BC, OC, CO₂, NH₃ and VOCs, respectively. Notably the emission fractions of point sources were larger than those in other regional inventories (Fu, 2009; Tang et al., 2012; B. Zhao et al., 2012), resulting mainly from the compiling and application of information on individual power and industrial plants from varied data sources. Defined as area source, open biomass burning contributed 12%, 19%, 23%, 11% and 41% to the total CO, PM₁₀, PM_{2.5}, BC and OC, respectively.

The dominant contributors to SO₂ were power plant, iron & steel and other industry, with the emission fractions estimated at 38%, 10% and 45%, respectively. Although the coal consumption in power sector was 3.5 times larger than that in other industry sector (cement and iron & steel production excluded, JSNBS, 2013), smaller contribution to SO₂ emissions were found for coal-fired power plants, implying the benefits of strict control on SO₂ emissions from power sector. As shown in Table S2, the application rate and average SO₂ removal efficiency of FGD in power sector were significantly higher than those in other industry, suggesting the improvement in SO₂ abatement for industrial coal combustion other than power plants would be an effective measure to further reduce the emissions at present.

Power sector was the largest source for NO_x, contributing 41% to the total emissions, while the share of coal consumption of the sector reached 65% (JSNBS, 2013). It thus implied the tightened controls from implementation of new emission standard (GB13223-2011) and improved use of SCR/SNCR on power plants since 2011 compared to other sectors. Compiled from unit level, the average NO_x removal efficiency of SCR/SNCR was calculated at 37% for Jiangsu's power plants in 2012 (Table S2), while Tian et al. (2013) estimated the values for SCR and SNCR at 70% and 25%, respectively, indicating the differences in assessment of emission controls for power sector between the provincial and national emission inventories with varied data sources. Transportation (including on-road and non-road) was estimated to be

the second largest sector for NO_x emissions, with the share to the total emissions calculated at 24%. Without specific control measures, cement and other industry were estimated to account for 7% and 18% of total NO_x emissions.

CO was mainly generated from the manufacturing processes in iron & steel plants. The production of pig iron and crude steel in Jiangsu accounted for 9% and 10% to the national total in 2012, respectively (NBS, 2013), and was higher than other provinces in China except Hebei. Due to the intensive iron & steel industry, the contribution of the sector to the provincial total CO emissions was estimated at 35%. Residential biofuel combustion, open biomass burning and on-road transportation were also large contributors to CO with the emission fractions calculated as 24%, 12% and 11% respectively.

For particles, iron & steel and cement production were estimated to be the largest sources, contributing 24% and 27% to the total emissions of PM₁₀, and 27% and 19% to PM_{2.5}, respectively. Even with the largest coal consumption among all the sectors, the emissions from power plants were relatively small (6% and 4% to the total PM₁₀ and PM_{2.5} emissions, respectively), resulting mainly from the relatively high penetrations and removal efficiencies of dust collectors. Great differences existed in the sector distribution of BC and OC emissions. Iron & steel was estimated to be the largest source of BC, while open biomass burning and biofuel burning in residential stoves dominated OC, with the shares estimated at 41% and 29%, respectively. Moreover, as BC exhausted from the diesel engines was demonstrated to be higher than OC in previous situ measurements (He et al., 2015), BC emissions from non-road transportation (agricultural machines, rural vehicles, ships and construction machines) was estimated more than twice larger than OC.

For VOCs, solvent use and other industry including oil refinery, chemical industry and combustion were identified as the largest sources contributing 30% and 29% to total emissions, respectively. In particular, oil refinery and chemical engineering collectively accounted for 74% of the emissions of other industry. Due to lack of investigation on chemical industry plants, the fraction of area sources to the emissions of other industry reached 35%. Transportation and residential cooking are estimated to contribute 12% and 4% to total VOCs emissions, respectively. Livestock and fertilizer use were the two dominating sources of NH₃, with the shares to total emissions estimated at 47% and 45%, respectively.

For industry, ammonia production was the main source accounting for half of NH₃ emissions.

The spatial distribution of SO₂, NO_x, CO, PM_{2.5}, VOCs and NH₃ emissions were at a resolution of 3×3km were illustrated in Figure S3 in the supplement. Outstandingly high emissions of SO₂, NO_x, PM_{2.5} and VOC indicated the existence of large industrial plants, particularly in Suzhou, Nanjing and Wuxi along with the Yangtze River. For CO and NO_x, large emissions were distributed along the road net in the province, reflecting the important contribution of on-road transportation. Unlike other pollutants, high NH₃ emissions were more evenly distributed in rural areas as dominated by agricultural activities.

3.2 Comparisons with other studies

Figure 3 compares the emission estimations for Jiangsu between our provincial inventory and previous studies including two regional inventories (Fu et al., 2013; Li et al., 2011) and two national ones (MEIC; Xia et al., 2016). Note this work and Xia et al. (2016) reported the numbers for 2012, while Fu et al. (2013), Li et al. (2011) and MEIC were for 2010. As the emissions from open biomass burning were not included in other inventories except Fu et al. (2013) and this work, two values labeled as A and B were provided for our provincial inventory indicating the emissions with and without biomass open burning, respectively. While provincial economy and energy data were generally applied in all the national/regional inventories, information of individual large emitters were incorporated as well in MEIC, Fu et al. (2013) and Li et al. (2011). For example, the emissions of big plants for power generation, iron & steel and cement production in Jiangsu were partially investigated in Fu et al. (2013) and Li et al. (2011). For MEIC, large fraction of emissions from power generation sector was calculated plant by plant with relatively good data availability, while emissions from other industrial sectors were basically calculated at regional average and spatially allocated as area sources. The results in Fu et al. (2013) were generally smaller than those in other two inventories for 2010.

Attributed mainly to the improved use of FGD, the total SO₂ emissions were estimated to decline from 2010 to 2012 for the whole country (Xia et al., 2016) and typical city in Jiangsu (Zhao et al., 2015). It was reasonable to some extent that the SO₂ emissions in Jiangsu estimated in this work for 2012 was less than the 2010 results of Li et al. (2011) and MEIC.

412 Our estimation was 15% lower than the result for Jiangsu extracted from the national
413 inventory by Xia et al. (2016), due mainly to the discrepancies in the penetration and SO₂
414 removal efficiency of FGD applied in the two inventories. Such information was obtained at
415 provincial or national average level by Xia et al. (2016), in contrast to the provincial
416 inventory based on investigation at plant level. For example, Xia et al. (2016) assumed that
417 the penetration rates of wet and dry FGD technologies in coal-fired power sector were 83%
418 and 5% in 2012, with the removal efficiencies estimated at 80% and 40%, respectively, and
419 that there was not any SO₂ control in the remaining 11% of installed capacity at all. According
420 to our plant-based investigation, the controls in Jiangsu were clearly enhanced, as shown in
421 Table S2. As a result, SO₂ emissions from power sector was calculated at 430.0 Gg for
422 Jiangsu 2012 in this work, 42% lower than those in Xia et al. (2016). The result for 2012 in
423 our provincial inventory, however, is very close to the estimation by MEIC for 2010 (437.4
424 Gg), even though the coal consumption of power generation increased 29% for the period
425 2010-2012 (JSNBS, 2013). Besides the uncertainty in emission estimation from varied data
426 sources of the two inventories, the improved use of FGD in the sector could be an important
427 reason for the restrained emissions. Similar fact was found for Nanjing, the capital city of
428 Jiangsu, that the SO₂ emissions of power generation calculated at city level kept stable along
429 with a 25% growth of coal consumption from 2010 to 2012 (Zhao et al., 2015).

430 NO_x emissions in our provincial inventory was slightly higher than those of Li et al.
431 (2011) and clearly lower than the two national inventories. The major difference between the
432 provincial inventory and MEIC was from industry, attributed probably to the application of
433 varied emission factors. With different methods and data sources for certain sectors, the NO_x
434 emissions from industry were calculated at 388.1 and 566.2 Gg respectively by this work and
435 Xia et al. (2016). For on-road transportation, the emission factors were estimated using
436 CORPERT in this work, while they were obtained from limited domestic measurements in
437 Xia et al. (2016). That was also the most important reason for the discrepancies in CO
438 emission estimation between the two studies. For 2010, the NO_x emissions estimated by Fu et
439 al. (2013) was 18% and 36% lower than those by Li et al. (2011) and MEIC, resulting mainly
440 from the higher application rate and removal efficiency of SCR/SNCR technologies for power
441 sector used in Fu et al. (2013).

442 The PM_{2.5} and PM₁₀ emissions in the provincial inventory were estimated to be 6% and
 443 23% higher than those of Xia et al. (2016), and the sector contributions were notably different
 444 in the two inventories. For example, industry was estimated to contribute 77% and 80% of
 445 PM_{2.5} and PM₁₀ in the provincial inventory, much larger than the fractions at 45% and 52% by
 446 Xia et al. (2016), respectively. In this work, the PM_{2.5} and PM₁₀ emissions from cement
 447 production were calculated at 181 and 384 Gg, i.e., 2.5 and 2.0 times to those in Xia et al.
 448 (2016), and the analogue numbers for iron & steel production were 134 and 263 Gg, and 1.8
 449 and 1.7 times, respectively. The discrepancies resulted mainly from the inconsistent
 450 penetration rates and removal efficiencies of dust collectors determined at national level and
 451 from on-site survey at provincial level. Taking cement as an example, all the plants were
 452 assumed to be installed with dust collectors, and the national average removal efficiency at
 453 99.3% was applied in Xia et al. (2016), clearly larger than that from plant-by-plant survey as
 454 shown in Table S2. Note that the particle emissions in the provincial inventory were estimated
 455 higher than those in national ones including MEIC and Xia et al. (2016), while the gaseous
 456 pollutant emissions were lower except for NH₃ and CO₂. Compared to the emissions for 2010
 457 estimated by other studies, the PM_{2.5} and PM₁₀ in our provincial inventory were 58% and 56%
 458 larger than Fu et al. (2013) (biomass open burning included), and 24% and 25% larger than Li
 459 et al. (2011) (biomass open burning excluded), respectively, beyond the growth rate of 20%
 460 for coal consumption during 2010-2012 (NBS, 2011; 2013).

删除的内容: It thus implied that the control of SO₂ and NO_x in Jiangsu were stronger than the average level at national scale investigated by Xia et al. (2016) but weaker for particles from power and industry sector.

461 The NH₃ emissions of Fu et al. (2013) and Li et al. (2011) were close to each other, while
 462 MEIC was only half of them for 2010. Using the results for 2006 from Huang et al. (2012),
 463 MEIC made a very low estimation in NH₃ emissions from livestock. The NH₃ emissions for
 464 2012 in this work was calculated 11% and 22% larger than the results for 2010 by Fu et al.
 465 (2013) and Li et al. (2011), respectively. According to the provincial statistics, the total
 466 numbers of livestock and poultry increased 6% and 10% from 2010 to 2012 in Jiangsu
 467 (JSNBS, 2013). The growth of activity levels was expected to result in enhanced emissions,
 468 as very little progress was achieved for NH₃ control for these years.

删除的内容: T

删除的内容: quantity

删除的内容: large animals

删除的内容: including cow, horse, sheep, goat, pig, donkey and mule

删除的内容: the weight of chicken (and duck) meat was also increased

删除的内容: Thus, t

469 3.3 Analysis of spatial distribution of emissions from given sectors

470 To further explore the discrepancies in emission estimation and spatial distribution from

varied data and emission allocation methods, comparisons between MEIC and our provincial inventory were conducted for pollutants from typical sources, including SO₂ from power plants, NO_x from transportation, and PM_{2.5} from industry. The estimates in this work were reallocated into the 0.25°×0.25° grids, consistent with the spatial resolution of MEIC, and the correlation coefficients for emissions in all the grids can be calculated, as shown in Figure 4. Due mainly to the relatively transparent and easily available information of power plants, good consistency was found for SO₂ emissions from power sector in the two inventories, with the correlation coefficient calculated at 0.7 (Figure 4a). Even though the fundamental information of power plants in China is more accessible than other industry sources, mismatches still exist in different data sources. For example, some emission hotspots in our provincial inventory were not totally identical with those in MEIC in Suzhou, Nantong and Nanjing. In contrast to plant-by-plant investigation, the data from existing statistics at national level could not fully track the actual changes in the emitters, e.g., operation of new-built units, shutting down the small ones, or relocation of individual plants. In MEIC, moreover, the SO₂ emissions in several grids were estimated extremely small (less than 1 Mg), indicating that part of emissions from power sector was still allocated as area sources based on density of GDP or population. In contrast, all the plants were identified as point sources in the provincial inventory, based on the thorough investigation on individual sources.

For NO_x from transportation, the correlation coefficient was calculated at 0.8, indicating an even better consistency than SO₂ from power plants between the two inventories (Figure 4b). Although the difference in total emissions was small between our provincial inventory (682 Gg) and MEIC (722 Gg), the estimation of MEIC was notably higher than our result for northern Jiangsu including Yancheng, Huai'an and Suqian, implying the impacts from different ways for emission allocation. In this work, emissions from on-road vehicles were calculated and allocated based on road net that incorporates the information of transportation flow by road grade for each city. For non-road sources, large fraction of emissions was allocated based on the GDP density incorporated with land-use type. In national emission inventories, however, the emissions were first calculated at provincial level, and then downscaled at certain horizontal resolution. Despite of the discrepancies, it could be indicated by the relatively high spatial correlation between the two inventories that using GDP as proxy

501 for emission allocation would be acceptable when detailed information on road net and
502 transportation flow was unavailable, since vehicles were largely concentrated in downtown
503 with the intensive economic activity.

504 For PM_{2.5} from industry, the correlation coefficient was calculated at 0.335, significantly
505 lower than those mentioned above, indicating larger discrepancy in spatial distribution of
506 industrial emissions between provincial and national inventories compared to power and
507 transportation sectors. As shown in Figure 4c, the emission hotspots in the provincial
508 inventory are highly consistent with the locations of large industrial PM_{2.5} emitters (more than
509 10 Gg) estimated in this work, while the emission in MEIC were more distributed in
510 developed cities (e.g., Suzhou) with high density of population or economy. Along with fast
511 urbanization, super industrial sources have gradually been relocated to the rural and suburban
512 areas, and the spatial correlation between industrial emissions and population could thus be
513 weakened. In our provincial inventory, most industrial enterprises were identified as point
514 sources, with the key parameters including geographic location, activity level and removal
515 efficiency of dust collector investigated and corrected at plant level. In MEIC, the emissions
516 were calculated using parameters at regional average level and allocated as area sources
517 according to densities of population and/or economic activity. Without detailed information
518 for individual sources, it might lead to errors in emission estimation and spatial distribution at
519 regional or local scale. According to the survey at plant level, for example, only 20% of the
520 lime factories were installed dust collectors in Jiangsu 2012, much lower than the value
521 (roughly 90%) assumed in national inventories. As a result, the PM_{2.5} emissions from industry
522 were calculated at 570 Gg in our provincial inventory, 78% higher than those of MEIC.

523

524 4 ASSESSMENT OF THE PROVINCIAL EMISSION INVENTORY

525 4.1 Evaluation of spatial distribution of NO_x emissions with satellite observation

526 Tropospheric NO₂ vertical column density (VCD) retrieved from Ozone Monitoring
527 Instrument (OMI) by the Royal Netherlands Meteorological Institute (Boersma et al., 2011)
528 was employed to test the spatial distribution of NO_x emissions in MEIC and this work.

529 Tropospheric NO₂ over China in this product is consistent with NO₂ data from ground-based

删除的内容: Troposphere

带格式的: 下标

带格式的: 下标

measurements with multi-axis DOAS ($R^2=0.96$; Lin et al., 2014). Since clouds reduce the accuracy of satellite measurements, only pixels with cloud fraction ≤ 0.2 have been analyzed.

NO₂ VCDs in summer were used due to the short lifetime of NO₂ in atmosphere at high temperature and the difficulty in accumulation for primary emissions with strong air convection. In addition, the summer prevailing wind for Jiangsu was generally from southeast where Shanghai and Zhejiang Province are located (see Figure S1 for the locations of the three regions). Total NO_x emissions of Jiangsu were estimated to be 65% and 282% larger

than those of Zhejiang and Shanghai in MEIC, indicating the local sources played an important role in the air pollution formation for the province (Cheng et al., 2011). As Mijling

删除的内容: dominated

删除的内容: level

et al. (2013) illustrated satellite observations could be used to evaluate the primary emissions for regions where NO₂ VCDs were mainly affected by local emissions, it was thus feasible to apply the OMI NO₂ VCDs in Jiangsu to assess its NO_x emissions.

NO₂ VCDs in July 2010 and 2012 with original spatial resolution of $0.125^\circ \times 0.125^\circ$ were used for comparisons with the emissions in MEIC and our provincial inventory, respectively. To be consistent with MEIC, the emissions in our provincial inventory and the NO₂ VCDs from OMI were first upscaled to $0.25^\circ \times 0.25^\circ$ for the purpose of visualization and correlation analysis. As can be seen in Figure 5a and 5b, clear reduction in summer NO₂ VCDs was found in southern Jiangsu from 2010 to 2012, indicating the benefits of efforts on NO_x abatement since 2011. The NO₂ VCDs in the area along the Yangtze River were notably higher than that in other regions, attributed possibly to the substantial emissions from vessels and small captive power plants of the chemical and refinery industrial parks along the river without stringent controls as big power plants. Shown in Figure 5c and 5d are the spatial distributions of Jiangsu's NO_x emissions in MEIC and our provincial inventory, respectively, and the emission hotspots were generally consistent between the two inventories. Figure 5e and 5f shows the linear regression results between NO₂ VCDs and NO_x emissions in MEIC and the provincial inventory, respectively. The correlation coefficients between VCDs and emissions were separately provided for all the grids and grids in different emission intervals, i.e., top 50%, 50%-75%, and last 25%.

The correlation coefficient between NO₂ VCDs and NO_x emissions from the provincial inventory was 0.534, close to that between NO₂ VCDs and MEIC at 0.531. The result

indicated that there was no significant difference in spatial distribution of emissions between the national and provincial inventories at the relatively low horizontal resolution. However, great discrepancies existed when the correlation analysis was conducted for grids in different emission intervals. As shown in Figure 5e, the correlation coefficients between VCDs and MEIC emissions were calculated at 0.24 and 0.34, respectively, for the top 50% (20 grids with emissions ranged 32-121 Gg) and last 25% of gridded emissions (161 grids with emissions ranged 0-12 Gg). For our provincial emission inventory, the correlation coefficients were estimated slightly higher at 0.28 and 0.38, respectively, for the top 50% (18 grids with emissions ranged from 30-75 Gg) and last 25% of gridded emissions (176 grids with emissions ranged 0-12 Gg). Moreover, the coefficient between NO₂ VCDs and gridded emissions for the 50% -75% interval in provincial inventory was 0.26, while negative value (-0.07) was calculated for MEIC, indicating that the emission estimation for areas with small and medium sources in the provincial inventory was more consistent with satellite observation. To better quantify the emissions at local scale, the results revealed the practical significance of careful investigation on individual small industrial sources that were usually identified as area sources due to lack of detailed information in national or regional inventories.

The comparisons between spatial distribution of VCDs and emissions should be interpreted cautiously, particularly for regions with relatively low values, as the noise to signal ratio in OMI NO₂ increases with decreased VCDs. Moreover, although summer data were applied to mitigate the effects of long lifetime of NO₂ on pollution plums transport and chemical reaction, non-linear relationship still exists between emissions and VCDs. More comparisons between NO₂ from satellite observation and CTM are thus recommended when improved characterization of NO₂ vertical distribution is available for the region.

4.2 Evaluation of multi-scale inventories with CMAQ

As mentioned in Section 2.5, anthropogenic emission inventories at provincial, regional and national scales were applied respectively to explore the impacts of emission input on the performance of city-scale air quality simulation using CMAQ. With the original horizontal resolutions at 0.25×0.25 and 4×4 km, respectively, national (MEIC) and YRD regional inventories (Fu et al., 2013) were reallocated into the D3 of CCTM modeling at 3×3km

589 (Figure 1), consistent with our provincial inventory. The vertical and temporal distributions of
590 the two inventories were assumed to be same as those of our provincial inventory, as indicated
591 in Section 2.4. For the simulation with provincial inventory, emissions inside and outside
592 Jiangsu in D3 were ~~taken~~ from the provincial inventory developed in this study and from the
593 reallocated YRD regional inventory by Fu et al. (2013), respectively. Given the very limited
594 data accessible on air quality for the province in 2012, the available observation data at nine
595 state-operated monitoring sites in Nanjing including six urban sites (Xuanwumen (XWM),
596 Shanxilu (SXL), Zhonghuamen (ZHM), Ruijinlu (RJL), Caochangmen (CCM), and
597 Maigaoqiao (MGQ)), and three suburban sites (Pukou (PKS), Xianlin (XLS) and Olympic
598 sports center (OSC)) were applied to evaluate the simulation performances with different
599 emission inputs (see locations of the nine sites in Figure 1).

删除的内容: adopted

删除的内容: ,

600 The hourly ground concentrations from observation and CMAQ simulation for October
601 2012, expressed as the averages for all the monitoring sites in Nanjing, were compared and
602 illustrated in Figure S4 in the supplement for SO₂, NO₂, ozone and PM_{2.5}. Even though all the
603 simulations could well reproduce the time variation of each species, discrepancies existed
604 when different anthropogenic emission inventory were used. The simulated SO₂ and NO₂
605 concentrations using the provincial inventory were notably lower than those with other two
606 inventories. In addition, simulations failed to catch the high PM_{2.5} and O₃ concentrations for
607 some heavy polluted episodes. For example, the average PM_{2.5} ground concentration during
608 October 21st-23rd and 28th-29th were simulated at 40 and 31 µg/m³, 1.4 and 3.2 times lower
609 than observations. Two statistical indicators, normalized mean bias (NMB) and normalized
610 mean error (NME), were applied to evaluate the model performance (Zhang et al., 2006), as
611 summarized in Table 2. Among all the species, the best simulation performance was found for
612 NO₂, with the NMBs ranged within ±30% for different emission. In general, simulations
613 using the provincial emission inventory performed notably better than those with national and
614 regional ones for all the species, and the NMEs and NMBs were calculated at 47%, 33%,
615 44%%, 52% and -10%, -14%, -25%, -43% for SO₂, NO₂, O₃, PM_{2.5} respectively, comparable
616 to previous U.S. studies (Zhang et al., 2006; Wang et al., 2009). The result thus partly
617 confirmed that air quality simulation at local or regional scales would be largely improved

when detailed information on individual sources could be incorporated in the emission inventory. Improved model prediction for pollution event was also achieved with provincial inventory. Taking the pollution episode between 8pm on 18th and 5pm on 19th October as an example, the observed PM_{2.5} concentration at CCM site kept increasing from 8pm on 18th with the highest value reaching 114 µg/m³ at 2am on 19th. Simulated PM_{2.5} concentrations with provincial, regional and national inventory at that time were 90, 53 and 45 µg/m³, respectively. The correlation coefficients between observation and simulations with the three inventories were calculated as 0.66, 0.44 and 0.30 during the episode, respectively, indicating the advantage of provincial inventory in the pollution event simulation.

Compared to primary pollutants SO₂ and NO₂, species with strong secondary formation process (PM_{2.5} and O₃ in this case) were clearly under predicted by CMAQ, no matter which inventory was applied. Lack of dust emissions in inventories might be one reason for underestimation of PM_{2.5}. Moreover, as the significant composition of PM_{2.5} in eastern China (Yang et al., 2011), secondary organic and inorganic aerosols might be under predicted attribute to the weakness of chemical mechanisms in the version of CMAQ including the transformation of sulfate and the formation of secondary organic aerosols (Wang et al., 2009). For ozone simulation, better performance was found at suburban sites than urban sites, and the lower simulated concentrations than observation could possibly come from the underestimation in precursor VOCs emissions. For example, the NMB was estimated at -26% for PKS, where many chemical industrial plants were located nearby. In addition, the uncertainty of NO_x emission estimation might also contribute to the discrepancy. As indicated by the data from available continuous emission monitoring systems on Jiangsu's power plants, the NO_x emission factors of power sector applied in current inventory might be overestimated for 2012 (unpublished).

The total emissions of SO₂ and NO_x in Jiangsu estimated by Fu et al. (2013) was 1126 and 1257 Gg, i.e., 9% and 22% lower than the results of our provincial inventory, respectively. Using the regional inventory by Fu et al. (2013), much higher concentrations of SO₂ and NO₂ were simulated than observation at the monitoring sites, with the NMBs calculated at 74% and 30%, respectively. Even with larger emissions, in contrast, the NMBs for simulation with

our provincial inventory were -10% and -14%, indicating lower simulated concentrations than observation. This result implies the possible impacts of spatial distributions of emissions on air quality modeling. In regional inventory, densities of population and economic activities were generally applied to allocate large fraction of emissions, leading to particularly high emissions in urban areas, as the economy and population was generally centralized in downtown. Given all the monitoring sites in Nanjing are located in urban or suburban areas, air quality simulation using regional emission inventory was thus liable to over predict the ground concentrations at those sites.

Spatial distributions of the monthly mean for simulated concentrations using national, regional and provincial inventories were plotted for SO₂, NO₂, PM_{2.5} and O₃ in Figure 6, and the differences between simulations with varied emissions were shown in Figure 7. As the MEIC emissions were greatly averaged when they were directly downscaled from 0.25°×0.25° to 3×3 km, the simulated high concentrations using MEIC were broadly distributed in the modeling domain and commonly located in downtown (as indicated in Figure S1), with the large emitters hardly identified (Figure 6a). For results using the regional and provincial inventories, there were several grids with notably outstanding simulated concentrations, indicating the existence of large emitters (Figure 6b and 6c), and differences with the simulation using MEIC were induced (Figure 7a and 7b). As shown in Figure 7c, moreover, clear differences were also detected between simulations using regional and provincial inventories, implying the discrepancy in allocations of high emissions between the two inventories. With the locations of large power, iron & steel, and cement plants incorporated, the YRD regional emission inventory by Fu et al. (2013) allocated a large fraction of emissions from industries as area sources. In contrast, the emissions from most power and industrial plants were calculated based on source-specific information and were precisely allocated in the provincial inventory, avoiding particularly the emission overestimation in downtown. In addition, the simulated NO₂ and O₃ concentrations for regions outside Jiangsu (i.e., Shanghai and part of Zhejiang and Anhui) using the provincial inventory were 22% lower and 40% higher in average than those using the regional one, respectively (Figure 7c), although same emissions (Fu et al., 2013) were used outside Jiangsu for the two inventories. The result indicates that both local and regional emissions were

important for the simulations of the secondary pollutant like O₃. Total VOCs emissions for Jiangsu were estimated at 1740 Gg in MEIC, slight higher than those in the regional (1659 Gg) and provincial inventory (1617 Gg), while the simulated monthly mean O₃ concentrations within Jiangsu using MEIC were notably lower than those using the latter two emissions. Categorized by CB05, differences in chemical compositions of VOCs could be found in the three inventories, attributed to the varied source contributions to VOC emissions and to the different source profiles used in emission speciation (Zhao et al., in preparation). For example, the emissions of ethane (ETH) and ethanol (ETHA) with relatively high ozone formation potential in the provincial inventory were 44% and 209% higher than those in MEIC, respectively. Therefore, the total emission amount, spatial distribution of emissions, and the chemical compositions of precursors are all crucial to the accuracy of ozone simulations, and further analysis on those factors are suggested.

4.3 Improved SO₂ simulation under special meteorological condition

To further examine the simulated concentration response to varied emission inputs at local scale, the simulated SO₂ concentrations using national, regional and provincial inventories were compared with observation at three monitoring sites in downtown Nanjing (XWH, RJL and ZHM) for 6th -14th October 2012, as illustrated in Figure 8. The simulated concentrations using our provincial inventory were the most consistent with observation, while apparent overestimation was found for the simulations using national or regional inventories. At 8 pm October 9 (local time), in particular, the SO₂ concentrations were observed at 33, 12, and 14 µg/m³ at XWH, RJL and ZHM sites, respectively, while the simulated concentrations were respectively simulated at 205, 246 and 228 µg/m³ using MEIC, i.e., 5-19 times higher than the observation. The analogue numbers with regional inventory by Fu et al. (2013) even reached 550, 477 and 476 µg/m³, i.e., 15-38 times higher than observation. Although concentrations remained over predicted, better performance was achieved when the improved provincial inventory was used, implying its advantage prior to national or regional ones in the high-resolution air quality modeling. The discrepancies in emissions and the simulated meteorological condition including wind velocity and height of planetary boundary layer (PBL) were inspected to understand the very high concentrations

from simulation.

Figure S5 in the supplement shows the simulated wind fields from 2 pm on 9th to 5am on 10th October. From 2 pm on 9th October 9, WS10 in downtown Nanjing started to decline gradually and reached the minimum of 0.22 m/s at 8 pm, simply not beneficial for the horizontal convection of atmosphere. In addition, the monthly average of PBL height at XWH was simulated at 485 m at day and 140 m at night in October. From 5pm on 9th to 10am on 10th, however, the average PBL height decreased to 39m, with the minimum simulated at 32 m at 11pm on 9th, seriously restricting the vertical diffusion of pollutants. Under the meteorological condition that horizontal and vertical movement of atmosphere were limited, primary pollutants from large emitters would be easily accumulated over time, possibly leading to high concentrations for areas close to the emission sources. In this case, therefore, the simulated SO₂ concentrations would be largely influenced by the emissions from local and nearby sources, as discussed below.

The total SO₂ emissions in Nanjing were estimated at 141 Gg in the provincial inventory, 2% and 7% higher than those of national and regional ones respectively. Without big difference in total amount, large discrepancies in spatial distribution existed in those inventories, particularly at high horizontal resolution as shown in Figure 9. Downscaled from 0.25°×0.25° to 3×3 km, grids with similar emissions were clustered for MEIC and spatial variations in emissions could hardly be detected other than the hotspot in downtown (Figure 9c). Notably lower emissions in downtown Nanjing were found in our provincial inventory than the regional one (Figure 9a and 9b). In addition, the grid with maximum SO₂ emissions (15.7 Gg) in the provincial inventory was in the northwestern of Nanjing where a super power plant was located, labeled as the black star (point A) in Figure 9. As a comparison, the grid with the maximum SO₂ emissions in the regional inventory labeled as the black triangle (point B) in Figure 9 was adjacent to the location of A, and its emissions were calculated to be only 28% of the result in the provincial one. Given no other super emitters located nearby, we expected that the discrepancy resulted mainly from the varied emission estimation and positioning for the same power plant in the two inventories. According to on-site survey, only one unit out of two for the plant was installed with FGD, and the SO₂ emissions of the plant was estimated at 13.6 Gg, accounting for 87% of the total emissions in the grid. In contrast, a

higher FGD installation rate at 85% was uniformly assumed for the power sector in the regional inventory by Fu et al. (2013), leading to possible underestimation in emissions for the plant. The comparison implied that detailed information compiled from individual plants were crucial for estimation and spatial distribution of pollutant emissions at local scales. SO₂ emissions at given monitoring sites were extracted from the gridded national, regional and provincial inventories and summarized in Table 3. As most large SO₂ emitters were located in suburban or rural areas, relatively small emissions were found in the provincial inventory for downtown Nanjing where the monitoring sites were located. As large fractions of emissions were allocated by the density of economy and population, however, the SO₂ emissions in the regional emission inventory were estimated at 1791, 1721, 1918, and 1635 Mg at XWH, RJL, ZHM and CCM sites, which were 4-5 times higher than those of our provincial inventory. In MEIC, the emissions at XWH, RJL, ZHM and MGQ sites were identically estimated at 1298 Mg from the downscaling approach, and they were also much larger than those in the provincial inventory. Given the unfavorable condition of pollutant transport for 9th-10th October, the overestimation in local emissions around the downtown monitoring sites in the national and regional inventories thus lead to terribly high simulated concentrations, while the results using the provincial one were much more reasonable. The comparison confirms the benefits of precise quantification of emissions on local air quality modeling.

Despite of significant improvement, overestimation in SO₂ concentrations still existed in the simulation with our provincial inventory, attributed possibly to the error of meteorology modeling. Here we selected XWH site as an example to conduct the back trajectory analysis using HYSPLIT model (<http://ready.arl.noaa.gov/HYSPLIT.php>). Shown in Figure S6 in the supplement, the air mass reaching the site at 50 m altitude came mainly from northeast at 11pm on 9th October. However, it was inconsistent with WRF modeling results, which indicated the dominating wind was from northwest (150°-170°) at that time. As mentioned above, a big power plant was located northwest to XWH (Figure 9a), and the site might partly be influenced by the large emissions from the plant and enhanced concentrations would then be obtained when northwest wind was simulated.

5 SENSITIVITY ANALYSIS OF PM_{2.5} AND OZONE FORMATION IN NANJING

Using the improved provincial inventory, the sensitivity of PM_{2.5} and O₃ concentrations to emissions were further analyzed through the Brute-Force method (BFM, Dunker et al., 1996). For PM_{2.5}, four simulation scenarios were designed: Scenario B (the base case) in which the emissions from all types of sources are included; and Scenarios S1, S2, and S3 in which the pollutant emissions of power, iron & steel and cement plants in D3 were zero out, respectively. The changes in simulated PM_{2.5} ground concentrations in S1, S2, and S3 compared to those in base case for October 2012 are illustrated in Figure S7 in the supplement. The average concentration increments in urban area of Nanjing caused by power, iron & steel, and cement plants were calculated respectively at 3, 11 and 7 µg/m³, accounting for 6%, 26% and 16% of the monthly mean PM_{2.5} concentrations, and the maximum increments within the domain reached 10, 72, and 25 µg/m³, respectively. Given the tiny emission fraction of power sector for primary PM_{2.5} (4% in Jiangsu Province) and the small share in the ground layers (15% for 1st plus 2nd vertical layers), its contribution to PM_{2.5} ground concentration was notably lower than those of iron & steel and cement. Summarized in Table 4 are the contributions of power, iron & steel, cement sectors to monthly mean PM_{2.5} at the nine monitoring sites in Nanjing, October 2012. The contributions of the three sectors to average PM_{2.5} concentrations at all the sites were estimated at 8%, 13% and 9%, respectively. Since all the sites are located in the urban or suburban areas, the estimated PM_{2.5} contributions at individual site varied slightly to each other. Besides monthly mean, the hourly maximum and minimum contributions are provided as well in Table 4. The largest hourly contributions from power, iron & steel and cement plants to PM_{2.5} concentrations were 65% at PKS, 89% at MGQ and 58% at both CCM and OCS, respectively. The contributions became negative at 2 pm on 26th October with average PM_{2.5} concentration of all the sites observed as 164 µg/m³ and simulated as 151 µg/m³ under the base case, i.e., increased particle concentrations were simulated at the moment when emissions from given sector was turned off. The result indicated, on one hand, the relatively high uncertainty of simulation for heavy PM pollution episode dominated by regional transport. On the other hand, as the simulated increments were mostly from the elevated sulfate (SO₄²⁻), nitrate (NO₃⁻) and ammonium (NH₄⁺), the negative

contributions might also be caused by the complex chemical mechanisms of SO₂ and NO_x reactions with NH₃ under the NH₃-rich condition in YRD (Wang et al., 2011). Intensive real-time observation on chemical composition of PM_{2.5} is thus recommended to better capture and analyze the processes.

To explore the sensitivity of O₃ formation to its precursor emissions, two scenarios were set besides the base case: the VOC-abatement scenario with 50% reduction of all anthropogenic VOCs emissions in D3 (Scenario P1), and the NO_x-abatement scenario with 50% reduction of NO_x in D3 (Scenario P2). Shown in Figure S8 in the supplement were the average O₃ concentration changes from October 6th to October 15th. The simulated O₃ average concentration from 11am to 5pm declined significantly under Scenario P1, with the maximum reduction at 54 µg/m³ (Figure S8a) within D3, and changes in the downwind region were greater than the upwind. In contrast, the concentrations were generally enhanced under P2 with the maximum increment at 19 µg/m³. Similar variation pattern was found for 1-hour maximum O₃ concentration in Figure S8b and monthly mean concentration in Figure S8c. The 1-hour maximum O₃ concentrations in most downwind area of Shanghai and southern Jiangsu decreased 10-20 µg/m³ with the reduction in VOCs emissions, and the concentrations would generally increase 10-30 µg/m³ with the NO_x reduction. The similar patterns of O₃ concentration variation in urban and downwind areas in D3 under P1 or P2 scenario indicated that the O₃ formation was VOCs-limited in all those areas in southern Jiangsu. Therefore, VOC emission abatement could be effective for O₃ pollution control in southern Jiangsu, while NO_x abatement might aggravate the pollution in autumn.

The temporal changes in the simulated O₃ concentrations between the P1/P2 and base scenarios at urban (XWH, SXL, RJL, MGQ, ZHM and CCM) and suburban sites (XLS, OCS and PKS) in Nanjing were illustrated for October 6th-16th in Figure 10. Simulated O₃ concentrations at urban and suburban sites were generally decreased once the VOC emissions declined and the maximum hourly reduction reached 77.3 and 49.6 µg/m³, respectively. In contrast, concentrations were elevated with the NO_x emission reduction and the maximum growth were 78.7 and 15.4 µg/m³, respectively. Under VOCs-limited regime, in general, the O₃ concentration would be little sensitive to the change of NO_x unless it was rich enough to turn to the negative correlation with O₃. Therefore, due to the intensive NO_x emissions from

on-road transportation in downtown Nanjing, the variations of O₃ concentrations in P2 scenario at urban monitoring sites were notably greater than those at suburban sites. It should be acknowledged that uncertainty existed in the analysis, as the brute-force method ignores the nonlinearity of O₃ response to the changes of precursor emissions. With techniques other than brute-force, e.g., ozone source apportionment (OSAT, Li et al., 2012) or tagged species method (Zhang et al., 2011), the nonlinearity mechanism of O₃ formation could be taken into account. Comparisons between results with different methods are further recommended for the region.

带格式的：下标

6 CONCLUSIONS

The bottom-up approach was applied to develop a high-resolution emission inventory for Jiangsu, with substantial detailed information on local sources incorporated. Key parameters relevant to emission estimation were examined and revised plant by plant including geographic position, energy consumption and removal efficiencies of APCD from various data sources and on-site survey on large emitters. Compared to previous studies, the emission fractions of point sources were significantly enhanced, except for NH₃ and OC, which are mainly from agriculture activities and biomass open burning, respectively. As lower removal efficiencies of dust collectors were obtained from local investigation, larger primary PM emissions were estimated in our provincial inventory than other national or regional ones. Moreover, clear discrepancy existed in spatial distribution of industrial PM_{2.5} emissions between this work and the national inventory MEIC, indicating the uncertainty of emission downscaling from coarse horizontal resolution. The spatial distribution of NO_x emissions in the provincial inventory was more consistent with summer tropospheric NO₂ VCDs observed from OMI than that of MEIC, particularly for the emissions from small and medium industrial plants. WRF-CMAQ air quality modeling system was set up to evaluate the reliability and improvement of the provincial emission inventory by comparing the simulation performance with that using a national (MEIC) and regional one. Among the three inventories, the best agreement was found between the observation and simulation with the provincial one for all the concerned species at the nine monitoring sites in Nanjing, while underestimation existed

particularly for PM_{2.5} and O₃ that were strongly influenced by secondary formation. Under the unfavorable meteorology of pollutant transport, extremely high SO₂ concentrations were simulated using the regional and national inventories, while the results using provincial one were much closer to the observation. The results indicated the advantage of improved estimation and spatial distribution of emissions on air quality modeling at regional or local scales. The improved provincial inventory was further applied for the sensitivity analysis on PM_{2.5} and O₃ formation using BFM simulation, and provided the preliminary results for the policy making of regional haze and photochemical pollution control in southern Jiangsu.

Limitations remained in the current inventory. Attributed to unavailability of detailed information, the weekly and hourly variation of emissions could not be fully tracked for each city, and the vertical distribution of emissions by sector, depending mainly on the stack height, temperature and flow of flue gas, could not be accurately determined. Instead, empirical data from previous work (Li et al., 2011; L. Wang et al., 2010; 2014) had to be applied, which might be inconsistent with the reality. In addition, some sources were not included in the current inventory, e.g., fugitive dust emissions from construction sites and road transportation, resulting from lack of reliable data and thereby potentially large uncertainties in the emission estimation at provincial level. Finally, the effects of source profiles on air quality modeling, e.g., the speciation of primary PM_{2.5} and VOC, were not fully evaluated. As they are important on the formation of O₃ and secondary particles, more investigations on typical sources and evaluation through chemistry transport modeling are suggested in the future.

ACKNOWLEDGEMENT

This work was sponsored by the Natural Science Foundation of China (41575142), Natural Science Foundation of Jiangsu (BK20140020), Jiangsu Science and Technology Support Program (SBE2014070918), and Special Research Program of Environmental Protection for Commonweal (201509004). We would like to acknowledge Litao Wang from Hebei University of Engineering, Jia Xing from Tsinghua University for the assistance in CMAQ model, and Xiao Fu from Tsinghua University for providing the emission inventory for Yangtze River Delta region, China.

882

883

REFERENCES

884 Baker: Meteorological modeling protocol for application to PM_{2.5}/haze/ozone modeling
885 projects, 2004.

886 Bo, Y., Cai, H., Xie, S. D.: Spatial and temporal variation of historical anthropogenic
887 NMVOCs emission inventories in China, *Atmos. Chem. Phys.*, 23, 7297-7316, 2008.

888 Boersma, K. F., Eskes, H. J., Dirksen, R. J., van der A, R. J., Veefkind, J. P., Stammes, P.,
889 Huijnen, V., Kleipool, Q. L., Sneep, M., Claas, J., Leitão, J., Richter, A., Zhou, Y., and
890 Brunner, D.: An improved tropospheric NO₂ column retrieval algorithm for the Ozone
891 Monitoring Instrument, *Atmos. Meas. Tech.*, 4, 1905–1928, doi:10.5194/amt-4-1905-2011,
892 2011.

893 Cai, H., Xie, S. D.: Estimation of vehicular emission inventories in China from 1980 to 2005,
894 *Atmos. Environ.*, 41, 8963-8979, 2007.

895 Cheng, Z., Chen, C. H., Huang, C., Huang, H. Y., Li, L., Wang, H. L.: Trans-boundary.
896 primary air pollution between cities in the Yangtze River Delta. *Acta Sci. Circum.*, 31,
897 686-694, 2011 (in Chinese).

898 Dong, Y. Q., Chen, C. H., Huang, C., Wang, H. L., Li, L., Dai, P., Jia, J. H.: Anthropogenic
899 emissions and distribution of ammonia in Yangtze River Delta, *Acta Sci. Circum.*, 29,
900 1611-1617, 2009 (in Chinese).

901 Dunker, A. M., Morris, R. E., Pollack, A. K., Schleyer, C. H., and Yarwood, G.:
902 Photochemical modeling of the impact of fuels and vehicles on urban ozone using auto oil
903 program data, *Environ. Sci. Technol.*, 30, 787–801, 1996.

904 EEA (European Environment Agency): COPERT 4-Computer Programme to Calculate
905 Emissions from Road Transport, User Manual (Version 9.0), Copenhagen, Denmark, 2012.

906 EEA (European Environment Agency): EMAP/CORINAIR Emission Inventory
907 Guidebook-2013, <http://www.eea.europa.eu/publications/emep-eea-guidebook-2013>, 2013.

908 Emery, C., Tai, E., Yarwood, G.: Enhanced meteorological modeling and performance
909 evaluation for two Texas episodes, Report to the Texas Natural Resources Conservation
910 Commission, prepared by ENVIRON, International Corp, Novato, CA, 2001.

911 Fu, J. Y., Jiang, D., Huang, Y. H.: 1Km Grid Population Dataset of China
912 (PopulationGrid_China), Global Change Research Data Publishing & Repository,
913 DOI:10.3974/geodb.2014.01.06. V1, 2014.

914 Fu, M. L., Ge, Y. S., Tan, J. W., Zeng, T., Liang, B.: Characteristics of typical non-road
915 machinery emissions in China by using portable emission measurement system, *Sci. Total*
916 *Environ.*, 437, 255-261, 2012.

917 Fu, Q. Y.: Emission inventory and the foundation mechanism of high pollution of fine
918 particulate matters in Shanghai (in Chinese), Ph. D thesis, Fudan University, Shanghai, China,

919 2009.

920 Fu, X., Wang, S. X., Zhao, B., Xing, J., Cheng, Z., Liu, H., and Hao, J. M.: Emission
 921 inventory of primary pollutants and chemical speciation in 2010 for the Yangtze River Delta
 922 region, China, *Atmos. Environ.*, 70, 39-50, 2013.

923 Han, K. M., Lee, S., Chang, L. S., and Song, C. H.: A comparison study between
 924 CMAQ-simulated and OMI-retrieved NO₂ columns over East Asia for evaluation of NOx
 925 emission fluxes of INTEX-B, CAPSS, and REAS inventories, *Atmos. Chem. Phys.*, 15,
 926 1913-1938, doi:10.5194/acp-15-1913-2015, 2015.

927 He, K. B.: Multi-resolution Emission Inventory for China (MEIC): model framework and
 928 1990–2010 anthropogenic emissions, International Global Atmospheric Chemistry
 929 Conference, 17–21 September, Beijing, China, 2012.

930 He, K. B. (eds): Guidebook of Air Pollutant Emission Inventory Development for Chinese
 931 Cities, Beijing, 2015 (in Chinese).

932 He, L. Q., Hu, J. N., Zu, L., Song, J. J., Chen, D.: Emission characteristics of exhaust PM_{2.5}
 933 and its carbonaceous components from China I to China III heavy-duty diesel vehicles, *Acta*
 934 *Scientiae Circumstantiae*, 35, 656-662, 2015 (in Chinese).

935 Huang, C., Chen, C. H., Li, L., Cheng, Z., Wang, H. L., Huang, H. Y., Streets, D. G., Wang,
 936 Y. J., Zhang, G. F., and Chen, Y. R.: Emission inventory of anthropogenic air pollutants and
 937 VOC species in the Yangtze River Delta region, China, *Atmos. Chem. Phys.*, 11, 4105-4120,
 938 2011.

939 Huang, R. J., Zhang, Y., Bozzetti, C., Ho, K. F., Cao, J. J., Han, Y., Daellenbach, K. R.,
 940 Slowik, J. G., Platt, S. M., Canonaco, F., Zotter, P., Wolf, R., Pieber, S. M., Bruns, E. A.,
 941 Crippa, M., Ciarelli, G., Piazzalunga, A., Schwikowski, M., Abbaszade, G., Schnelle- Kreis,
 942 J., Zimmermann, R., An, Z., Szidat, S., Baltensperger, U., Haddad, I. E., and Prevot, A. S.:
 943 High secondary aerosol contribution to particulate pollution during haze events in China,
 944 *Nature*, 514, 218–222, 2014.

945 Huang, X., Song, Y., Li, M. M., Li, J. F., Huo, Q., Cai, X. H., Zhu, T., Hu, M., and Zhang, H.
 946 S.: A high-resolution ammonia emission inventory in China *Global Biogeochem. Cycles*, 26:
 947 GB1030, doi:10.1029/2011GB004161, 2012.

948 Huang, Y. H., Jiang, D., Fu, J. Y.: 1Km Grid GDP Data of China (2005, 2010)
 949 (GDPGrid_China), Global Change Research Data Publishing & Repository,
 950 DOI:10.3974/geodb.2014.01.07. V1, 2014.

951 Huo, H., Wang, M., Zhang, X. L., He, K. B. Gong, H. M., Jiang, K. J., Jin, Y. F., Shi, Y. D., Yu
 952 X.: Projection of energy use and greenhouse gas emissions by motor vehicles in China: Policy
 953 options and impacts, *Energ. Policy*, 43: 37-48, 2012.

954 JSNBS (Jiangsu Bureau of Statistics): Statistical Yearbook of Jiangsu, Beijing, China
 955 Statistics Press, 2011 (in Chinese).

956 JSNBS (Jiangsu Bureau of Statistics): Statistical Yearbook of Jiangsu, Beijing, China

957 Statistics Press, 2013 (in Chinese).

958 Kain, J.: The Kain-Fritsch convective parameterization: An update, *J. Appl. Meteor.*, 43,
959 170-181, 2004.

960 Kurokawa, J., Ohara, T., Morikawa, T., Hanayama, S., Janssens-Maenhout, G., Fukui, T.,
961 Kawashima, K., and Akimoto, H.: Emissions of air pollutants and greenhouse gases over
962 Asian regions during 2000–2008: Regional Emission inventory in Asia (REAS) version 2,
963 *Atmos. Chem. Phys.*, 13, 11019–11058, doi:10.5194/acp-13-11019-2013, 2013.

964 Lei, Y., Zhang, Q., Nielsen, C., He, K. B.: An inventory of primary air pollutants and CO₂
965 emissions from cement production in China, 1990-2020, *Atmos. Environ.*, 45, 147-154, 2011.

966 Li, L., Chen, C. H., Fu, J. S., Huang, C., Streets, D. G., Huang, Y. H., Zhuang, G. F., Wang, J.
967 Y., Jang, C. J., Wang, H. L., Chen, Y. R., and Fu, M. J.: Air quality and emissions in the
968 Yangtze River Delta, China, *Atmos. Chem. Phys.*, 11, 1621-1639,
969 doi:10.5194/acp-11-1621-2011, 2011.

970 Li, M., Zhang, Q., Streets, D. G., He, K. B., Cheng, Y. F., Emmons, L. K., Huo, H., Kang, S.
971 C., Lu, Z., Shao, M., Su, H., Yu, X., and Zhang, Y.: Mapping Asian anthropogenic emissions
972 of non-methane volatile organic compounds to multiple chemical mechanisms, *Atmos. Chem.*
973 *Phys.*, 14, 5617-5638, 2014.

974 Lin, J., Martin, R. V., Boersma, K. F., Sneep, M., Stammes, P., Spurr, R., Wang, P., van
975 Roozendaal, M., Clémer, K., and Irie, H.: Retrieving tropospheric nitrogen dioxide from the
976 Ozone Monitoring Instrument: effects of aerosols, surface reflectance anisotropy, and vertical
977 profile of nitrogen dioxide, *Atmos. Chem. Phys.*, 14, 1441-1461, 2014

978 Ministry of Environmental Protection (MEP): China National Ambient Air Quality Standards,
979 GB3095-2012, MEP, Beijing, China, 2012 (in Chinese).

980 Mijling, B., Vander, A. R. J., Zhang, Q.: Regional nitrogen oxides emission trends in East
981 Asia observed from space, *Atmos. Chem. Phys.*, 13: 12003-12012, 2013.

982 National Bureau of Statistics (NBS): China Statistical Yearbook 2013, China Statistics Press,
983 Beijing, 2013a (in Chinese).

984 National Bureau of Statistics (NBS): China Industry Economy Statistical Yearbook 2012,
985 China Statistics Press, Beijing, 2013b (in Chinese).

986 National Bureau of Statistics (NBS): China Energy Statistical Yearbook 2012, China Statistics
987 Press, Beijing, 2013c (in Chinese).

988 Ohara, T., Akimoto, H., Kurokawa, J., Horii, N., Yamaji, K., Yan, X., and Hayasaka, T.: An
989 Asian emission inventory of anthropogenic emission sources for the period 1980–2020,
990 *Atmos. Chem. Phys.*, 7, 4419–4444, doi:10.5194/acp-7-4419-2007, 2007.

991 Price, C., Penner, J. and Prather, M.: NO_x from lightning, Part I: Global distribution based on
992 lightning physics, *J. Geophys. Res. Atmos.*, 102, D5, DOI: 10.1029/96JD03504, 1997.

993 Sindelarova, K., Granier, C., Bouarar, I., Guenther, A., Tilmes, S., Stavrou, T., Müller, J.-F.,

994 Kuhn, U., Stefani, P., and Knorr, W.: Global dataset of biogenic VOC emissions calculated by
 995 the MEGAN model over the last 30 years, *Atmos. Chem. Phys. Discuss.*, 14, 10725-10788,
 996 doi:10.5194/acpd-14-10725-2014, 2014.

997 Streets, D. G., Bond, T. C., Carmichael, G. R., Fernandes, S. D., Fu, Q., He, D., Klimont, Z.,
 998 Nelson, S. M., Tsai, N. Y., Wang, M. Q., Woo, J.-H., and Yarber, K. F.: An inventory of
 999 gaseous and primary aerosol emissions in Asia in the year 2000, *J. Geophys. Res.*, 108, 8809,
 1000 doi:10.1029/2002JD003093, 2003.

1001 Street, D. G., Fu, J. S., Jang, C. J., Hao, J. M., He, K. B., Tang, X. Y., Zhang, Y. H., Wang, Z.
 1002 F., Li, Z. P., Zhang, Q., Wang, L. T., Wang, B. Y., Yu, C.: Air quality during the 2008
 1003 Beijing Olympic Games, *Atmos. Environ.*, 41, 480-492, 2007.

1004 Tang, X. L., Zhang, Y., Yi, H. H., Ma J. Y., Pu L.: Development a detailed inventory
 1005 framework for estimating major pollutants emissions inventory for Yunnan Province, China,
 1006 *Atmos. Environ.*, 57, 116-125, 2012.

1007 Tian, H. Z., Liu, K. Y., Hao, J. M., Wang, Y., Gao, J. J., Qiu, P. P., and Zhu, C. Y.: Nitrogen
 1008 oxides emissions from thermal power plants in China: Current status and future predictions,
 1009 *Environ. Sci. Technol.*, 47, 11350-11357, 2013.

1010 Wang, K., Zhang, Y., Jang, C., Phillip, S., and Wang, B.Y.: Modeling intercontinental air
 1011 pollution transport over the trans-Pacific region in 2001 using the Community Multi scale Air
 1012 Quality modeling system, *J. Geophys. Res. Atmos.*, 114, D04307,
 1013 doi:10.1029/2008JD010807, 2009.

1014 Wang, Q. D., Huo, H., He, K. B., Yao, Z. L., Zhang, Q.: Characterization of vehicle driving
 1015 patterns and development of driving cycles in Chinese cities, *Transportation research part D:*
 1016 *transport and environment*, 13, 289-297, 2008.

1017 Wang, S. X., Zhao, M., Xing, J., Wu, Y., Zhou, Y., Lei, Y., He, K. B., Fu, L. X., and Hao, J.
 1018 M.: Quantifying the air pollutants emission reduction during the 2008 Olympic Games in
 1019 Beijing, *Environ. Sci. Technol.*, 44, 2490-2496, 2010.

1020 Wang, S. X., Xing, J., Jang, C. J., Zhu, Y., Fu, J. S., Hao, J. M.: Impact assessment of
 1021 ammonia emissions on inorganic aerosols in east China using response surface modeling
 1022 technique, *Environ. Sci. Technol.*, 45: 9293-9300, 2011.

1023 Wang, L. T., Jang, C., Zhang, Y., Wang, K., Zhang, Q., Streets, D. G., Fu, C. J., Lei, Y.,
 1024 Schreifels, J., He, K. B., Hao, J. M., Lam, Y. F., Lin, J., Meskhidze, N., Voorhees S., Evarts
 1025 D., Phillips S.: Assessment of air quality benefits from national air pollution control policies
 1026 in China. Part II: Evaluation of air quality predictions and air quality benefits assessment.
 1027 *Atmos. Environ.*, 44, 3449-3457, 2010.

1028 Wang, L. T., Wei, Z., Yang, J., Zhang, Y., Zhang, F. F., Su, J., Meng, C. C., and Zhang, Q.:
 1029 The 2013 severe haze over southern Hebei, China: model evaluation, source apportionment,
 1030 and policy implications, *Atmos. Chem. Phys.*, 14, 3151–3173, doi:10.5194/acp-14-3151-2014,
 1031 2014.

1032 Wei, W., Wang, S. X., Chatani, S., Klimont, Z., Cofala, J., and Hao, J. M.: Emission and

1033 speciation of non-methane volatile organic compounds from anthropogenic sources in China,
 1034 Atmos. Environ., 42, 4976–4988, 2008.

1035 Xia, S. J., Zhao, Q. Y., Li, B., Shen, G. F.: Anthropogenic source VOCs emission inventory
 1036 of Jiangsu Province, Research of Environmental Sciences, 27, 120-126, 2014 (in Chinese).

1037 Xia, Y. M., Zhao, Y., Nielsen, C. P.: The benefits of China's efforts in gaseous pollutant
 1038 control indicated by the bottom-up emissions and satellite observations, Atmos. Environ., 136,
 1039 43-53, 2016.

1040 Xing, J., Zhang, Y., Wang, S. X., Liu, X. H., Cheng, S. H., Zhang, Q., Chen, Y. S., Streets, D.
 1041 G., Jang, C. J., Hao, J. M., Wang, W. X.: Modeling study on the air quality impacts from
 1042 emission reductions and a typical meteorological conditions during the 2008 Beijing
 1043 Olympics, Atmos. Environ., 45, 1786-1798, 2011.

1044 Yang, F., Tan, J., Zhao, Q., Du Z., He, K., Ma, Y., Duan, F., Chen, G., and Zhao, Q.:
 1045 Characteristics of PM_{2.5} speciation in representative megacities and across China, Atmos.
 1046 Chem. Phys., 11, 5207-5219, doi:10.5194/acp-11-5207-2011, 2011.

1047 Ye, S. Q., Zheng, J. Y., Pan, Y. Y., Wang, S. S., Lu, Q., and Zhong, L. J.: Marine emission
 1048 inventory and its temporal and spatial characteristics in Guangdong Province, Acta Sci.
 1049 Circum., 34, 537–547, 2014 (in Chinese).

1050 Yin, S. S., Zheng, J. Y., Zhang, L. J., and Zhong, L. J.: Anthropogenic ammonia emission
 1051 inventory and characteristic in the Pearl River Delta region, Environ. Sci., 31, 1146–1151,
 1052 2010 (in Chinese).

1053 Yin, S. S., Zheng, J. Y., Lu, Q., Yuan, Z. B., Huang, Z. J., Zhong, L. J., Lin, H.: A refined
 1054 2010-based VOC emission inventory and its improvement on modeling regional ozone in the
 1055 Pearl River Delta Region, China, Sci. Total Environ., 514, 426-438, 2015.

1056 Zhang, H. L., Li, J. Y., Ying, Q., Yu, J. Z., Wu, D., Cheng, Y., He, K. B., Jiang, J. K.: Source
 1057 apportionment of PM_{2.5} nitrate and sulfate in China using a source-oriented chemical transport
 1058 model, Atmos. Environ., 62, 228-242, 2012.

1059 Zhang, L. J., Zheng, J. Y., Yin, S. S., Peng, K., and Zhong, L. J.: Development of non-road
 1060 mobile source emission inventory for the Pearl River Delta region, Environ. Sci., 31, 886-891,
 1061 2010 (in Chinese).

1062 Zhang, Q., Streets, D. G., Carmichael, G. R., He, K., Huo, H., Kannari, A., Klimont, Z., Park,
 1063 I., Reddy, S., Fu, J. S., Chen, D., Duan, L., Lei, Y., Wang, L., and Yao, Z.: Asian emissions in
 1064 2006 for the NASA INTEX-B mission, Atmos. Chem. Phys., 9, 5131-5153,
 1065 doi:10.5194/acp-9-5131-2009, 2009.

1066 Zhang, Y. and Carmichael, G. R.: The role of mineral aerosol in tropospheric chemistry in
 1067 East Asia-a model study, J. Appl. Meteorol., 38, 353-366, 1999.

1068 Zhang, Y., Liu, P., Pun, B., Seigneur, C.: A comprehensive performance evaluation of
 1069 MM5-CMAQ for the Summer 1999 Southern Oxidants Study episode-Part I: Evaluation
 1070 protocols, databases, and meteorological predictions, Atmos. Environ., 40, 4825-4838, 2006.

1071 Zhang, Y., Wang, W., Wu, S.-Y. Wang, K., Minoura, H., Wang, Z. F.: Impacts of updated
 1072 emission inventories on source apportionment of fine particle and ozone over the southeastern
 1073 U.S., *Atmos. Environ.*, 88, 133-154, 2014.

1074 Zhao, B., Wang, P., Ma, J. Z., Zhu, S., Pozzer, A., and Li, W.: A high-resolution emission
 1075 inventory of primary pollutants for the Huabei region, China, *Atmos. Chem. Phys.*, 12,
 1076 481-501, doi:10.5194/acp-12-481-2012, 2012.

1077 Zhao, B., Wang, S. X., Dong, X. Y., Wang, J. D., Duan, L., Fu, X., Hao, J. M., and Fu, J. S.:
 1078 Environmental effects of the recent emission changes in China: implications for particulate
 1079 matter pollution and soil acidification, *Environ. Res. Lett.*, 8, 24-31, 2013.

1080 Zhao, Y., Wang, S.X., Duan, L., Lei, Y., Cao, P.F., and Hao, J.M.: Primary air pollutant
 1081 emissions of coal-fired power plants in China: current status and future prediction. *Atmos.*
 1082 *Environ.*, 42, 8442-8452, 2008.

1083 Zhao, Y., Wang, S. X., Nielsen, C. P., Li, X. H., and Hao, J. M.: Establishment of a database
 1084 of emission factors for atmospheric pollutants from Chinese coal-fired power plants, *Atmos.*
 1085 *Environ.*, 44, 1515-1523, 2010.

1086 Zhao, Y., Nielsen, C. P., McElroy, M. B., Zhang, L., and Zhang, J.: CO emissions in China:
 1087 uncertainties and implications of improved energy efficiency and emission control, *Atmos.*
 1088 *Environ.*, 49, 103-113, 2012a.

1089 Zhao, Y., Nielsen, C. P., and McElroy, M. B.: China's CO₂ emissions estimated from the
 1090 bottom up: Recent trends, spatial distributions, and quantification of uncertainties, *Atmos.*
 1091 *Environ.*, 59, 214-223, 2012b.

1092 Zhao, Y., Zhang, J., Nielsen, C. P.: The effects of recent control policies on trends in
 1093 emissions of anthropogenic atmospheric pollutants and CO₂ in China, *Atmos. Chem. Phys.*,
 1094 13, 487-508, 2013.

1095 Zhao, Y., Qiu, L. P., Xu, R. Y., Xie, F. J., Zhang, Q., Yu, Y. Y., Nielsen, C. P., Qin, H. X.,
 1096 Wang, H. K., Wu, X. C., Li, W. Q., and Zhang, J.: Advantages of a city-scale emission
 1097 inventory for urban air quality research and policy: the case of Nanjing, a typical industrial
 1098 city in the Yangtze River Delta, China, *Atmos. Chem. Phys.*, 15, 12623-12644,
 1099 doi:10.5194/acp-15-12623-2015, 2015.

1100 Zhao, Y., Mao, P., Zhou, Y., Yang, Y., Zhang, J., Wang, S., Dong, Y., Xie, F., Yu, Y., and Li,
 1101 W.: Improved provincial emission inventory and speciation profiles of anthropogenic
 1102 non-methane volatile organic compounds: a case study for Jiangsu, China, in preparation.

1103 Zheng, J. Y., Zhang, L. J., Che, W. W., Zheng, Z., and Yin, S. S.: A highly resolved temporal
 1104 and spatial air pollutant emission inventory for the Pearl River Delta region, China and its
 1105 uncertainty assessment, *Atmos. Environ.*, 43, 5112-5122, 2009.

1106 Zheng, J. Y., Fu, F., Li, Z. C., Wang, S. S., Zhong, L. J.: Implementation and evaluation of
 1107 uncertainty propagation using stochastic response surface method based on the CMAQ model,
 1108 *Acta Sci. Circum.*, 32, 1289-1298, 2012 (in Chinese).

FIGURE CAPTIONS

Figure 1. Modeling domain and locations of 43 meteorological and 9 air quality monitoring sites.

Figure 2. Source contributions to total estimated emissions by species in Jiangsu 2012. Colors indicate the sectors and the shade patterns indicate the source type (point, mobile and area).

Figure 3. Comparison between the emissions estimated in this work and other studies for Jiangsu. A and B indicate the emissions without and with open biomass burning, respectively.

Figure 4. Spatial distributions (a-c) and linear regression (d) of certain pollutant emissions from typical sources estimated in our provincial inventory and MEIC. (a) SO₂ from power plant; (b) NO_x from transportation; (c) PM_{2.5} from industry. The black points indicate the locations of plants with PM_{2.5} emissions larger than 10 Gg estimated in this work.

Figure 5. Spatial distributions of NO₂ VCDs observed by OMI in Jiangsu in 2010 (a) and 2012 (b), and those of Jiangsu's NO_x emissions from MEIC (c) and our provincial inventory (d) at the resolution of 0.25°×0.25°. Linear regressions of gridded VCDs and emissions are illustrated for MEIC (e) and our provincial inventory (f).

Figure 6. Spatial distributions of the monthly means of simulated SO₂, NO₂, PM_{2.5} and O₃ concentrations using the national, regional and provincial emission inventories for October 2012.

Figure 7. The differences in the monthly means of simulated SO₂, NO₂, PM_{2.5} and O₃ concentrations using different emission inventories: (a) Provincial–national; (b) Regional–national; and (c) provincial–regional. The black star A and triangle B referred to the locations of grids with maximum SO₂ emissions in provincial and regional inventory.

Figure 8. The observed and simulated hourly SO₂ concentrations (expressed with 3-h interval) using the national, regional, and provincial inventories at XWH (a), RJL (b), and ZHM (c) from October 6th to 13th, 2012.

Figure 9. Spatial distributions of the estimated SO₂ emissions in Nanjing at the resolution of 3×3km in the provincial (a), regional (b) and national emission inventory (c). The black dots indicate the locations of given air quality monitoring sites. The black star (point A) indicates the location of the power plant with the largest SO₂ emissions estimated in the provincial inventory. The black triangle (point B) indicates the speculated position of the same power plant in the regional inventory.

Figure 10. The changes in simulated O₃ concentrations at urban (XWH, SXL, RJL, MGQ, ZHM, and CCM) and suburban air quality monitoring sites (XLS, OSC, and PKS) in Nanjing under P1 (a) and P2 (b) scenarios compared to the base case for 6th-16th October 2012.

TABLES

Table 1. The estimated annual emissions by city for Jiangsu 2012 (unit: million metric tons (Tg) for CO₂ and kilo metric tons (Gg) for other species).

City	SO ₂	NO _x	CO	TSP	PM ₁₀	PM _{2.5}	BC	OC	CO ₂	NH ₃	VOCs
Southern											
Nanjing	140.6	210.5	742.9	157.3	97.3	75.8	5.8	7.1	97.1	64.2	221.9
Suzhou	220.8	286.7	1383.3	380.6	194.9	137.3	9.8	11.0	184.4	144.8	297.8
Wuxi	107.7	180.0	545.5	271.3	126.9	77.2	3.4	9.6	84.5	24.2	167.2
Changzhou	104.0	107.7	734.6	413.3	194.6	126.2	3.6	7.5	65.2	33.4	104.2
Zhenjiang	44.0	89.6	231.6	143.3	66.8	40.9	1.9	6.6	53.0	38.1	55.4
Central											
Nantong	76.8	130.1	443.4	244.9	108.2	66.0	4.8	9.3	51.6	181.7	162.2
Yangzhou	55.3	93.9	310.7	54.1	39.9	31.1	2.6	8.5	52.1	83.1	82.5
Taizhou	56.6	70.5	315.1	207.6	98.2	52.3	2.7	8.8	31.4	100.7	76.9
Northen											
Xuzhou	138.9	232.5	805.5	223.2	146.5	101.9	6.1	19.1	139.2	49.2	161.2
Huai'an	52.2	61.5	590.0	97.4	64.5	49.5	3.7	12.0	32.5	195.9	78.6
Yancheng	49.9	78.5	639.7	203.8	111.8	72.0	5.6	16.1	28.2	101.0	185.0
Lianyungang	60.6	61.0	571.1	131.0	89.0	68.6	3.9	11.9	28.3	25.1	78.0
Suqian	34.1	39.7	366.8	77.8	55.5	42.3	3.2	11.0	12.9	59.1	76.4
Total	1141.5	1642.2	7680.0	2605.6	1394.0	941.1	57.0	138.5	860.5	1100.3	1747.3

Table 2. Model performance statistics for concentrations of given species from observation and CMAQ simulation using the national, regional and provincial inventories at the nine air quality monitoring sites in Nanjing for October 2012.

Pollutants	National (MEIC)		Regional (Fu et al., 2013)		Provincial (this work)	
	NMB	NME	NMB	NME	NMB	NME
SO ₂	48.45%	76.53%	74.08%	95.04%	-9.97%	47.49%
NO ₂	21.02%	35.99%	29.84%	43.45%	-14.47%	33.22%
O ₃	-65.55%	68.57%	-53.93%	61.59%	-24.98%	44.29%
PM _{2.5}	-51.63%	55.32%	-49.16%	56.00%	-43.64%	51.81%

Note: NMB and NME were calculated using following equations (P and O indicate the results from modeling prediction and observation, respectively):

$$NMB = \frac{\sum_{i=1}^n (P_i - O_i)}{\sum_{i=1}^n O_i} \times 100\%; \quad NME = \frac{\sum_{i=1}^n |P_i - O_i|}{\sum_{i=1}^n O_i} \times 100\%$$

Table 3. The annual SO₂ emissions estimated in three inventories at given air quality monitoring sites in downtown Nanjing.

SO ₂ /Mg	National (MEIC)	Regional (Fu et al., 2013)	Provincial (this work)
XWH	1297.5	1790.9	411.0
RJL	1297.5	1720.8	303.1
ZHM	1297.5	1918.3	396.2
CCM	928.6	1635.3	371.8
MGQ	1297.5	478.6	395.0

Table 4. The monthly mean contributions of power, iron & steel and cement plants to the PM_{2.5} concentrations at the air quality monitoring sites in Nanjing in October 2012.

Monitoring site	Contri. of power (%)			Contri. of iron & steel (%)			Contri. of cement (%)		
	Max.	Min.	Ave.	Max.	Min.	Ave.	Max.	Min.	Ave.
XWH/SXL	52	-6	8	82	-2	14	43	-1	8
RJL	42	-6	7	79	0	11	44	0	9
ZHM	44	-5	7	71	-3	12	48	0	9
CCM	32	-8	7	83	-4	13	58	-5	8
MGQ	58	-5	9	89	-2	8	35	-5	7
XLS	35	-5	7	67	-3	10	57	0	10
PKS	65	-6	7	77	-1	11	45	-1	7
OCS	33	-7	7	87	0	12	58	0	8

Note: Max., min., ave. and contri. indicate maximum, minimum, average and contribution, respectively.

Figure 1

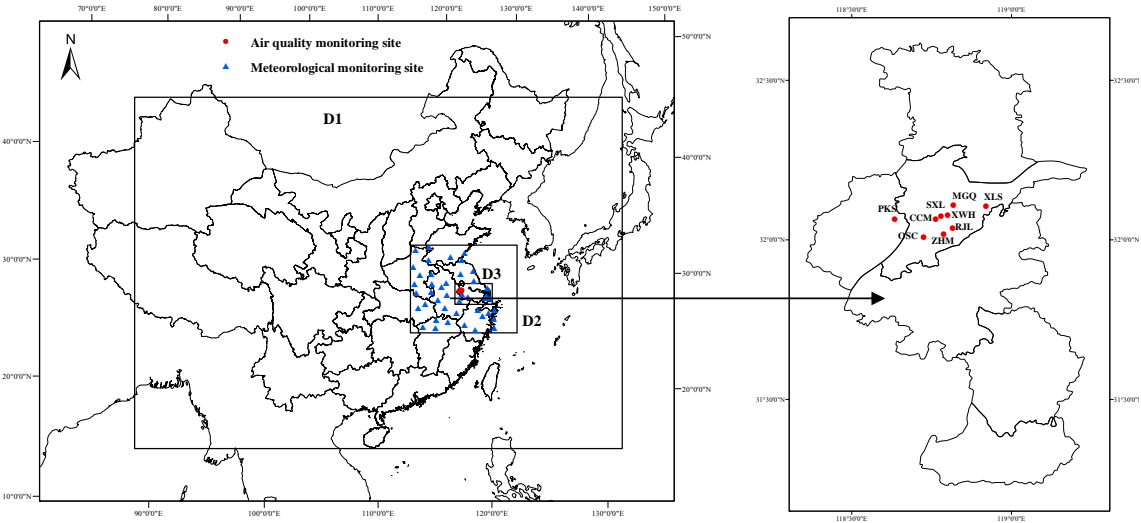


Figure 2

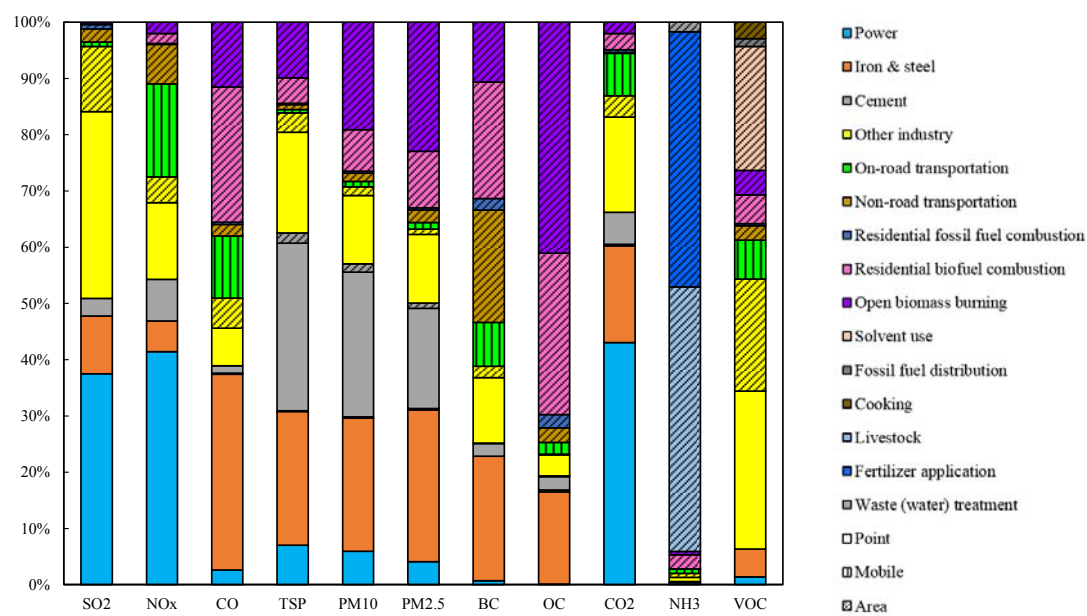


Figure 3

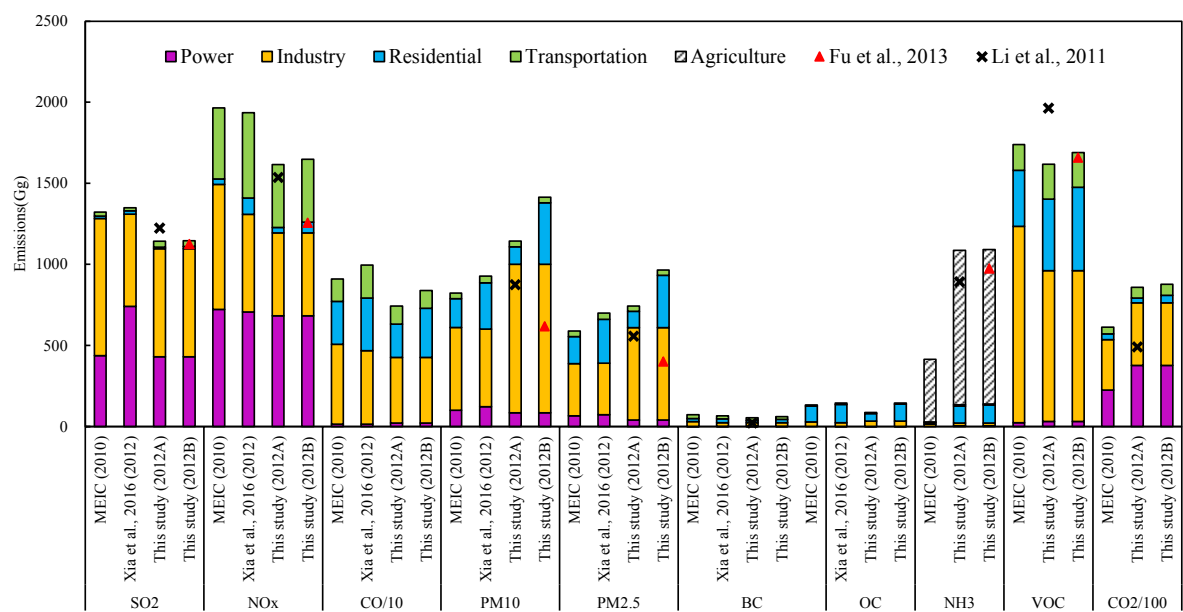


Figure 4

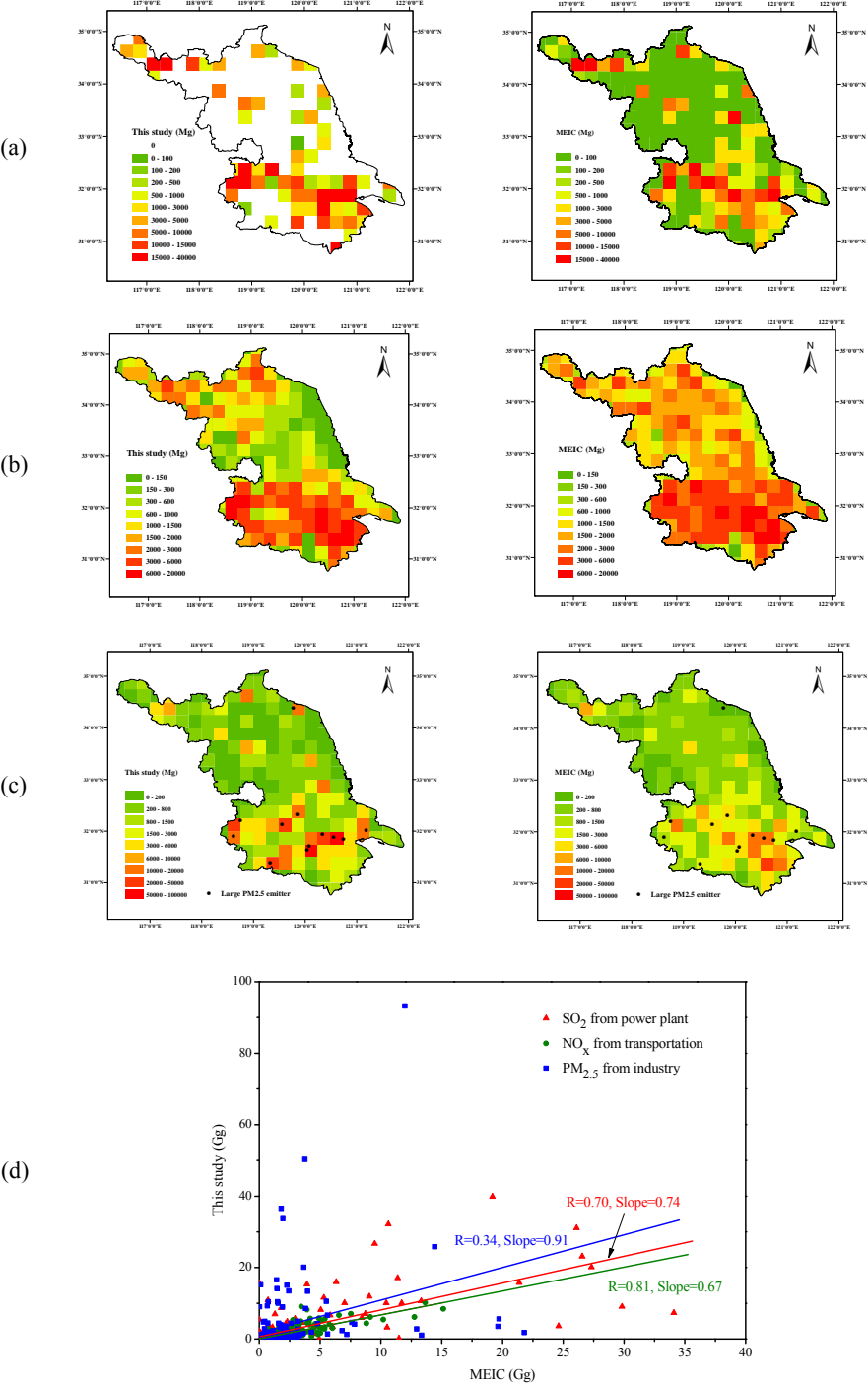


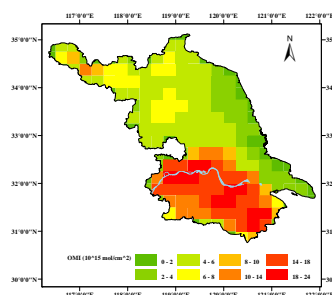
Figure 5

NO₂ VCDs

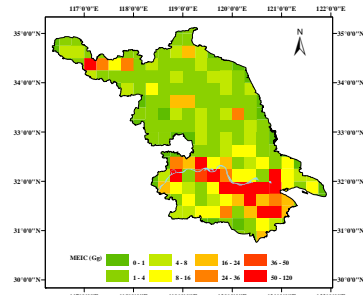
NO_x emission

Linear regression

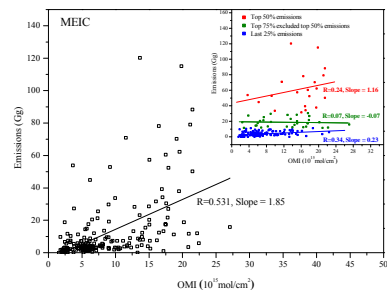
2010



(a)

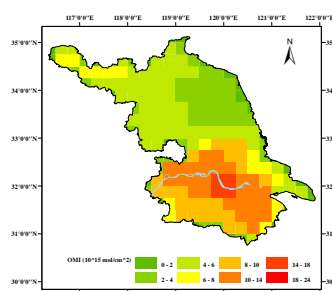


(c)

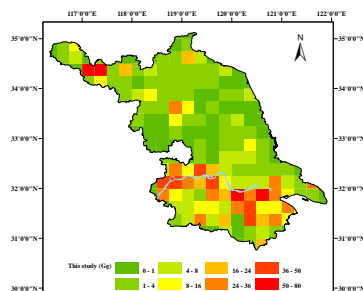


(e)

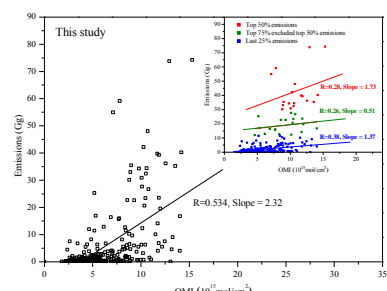
2012



(b)



(d)



(f)

Figure 6

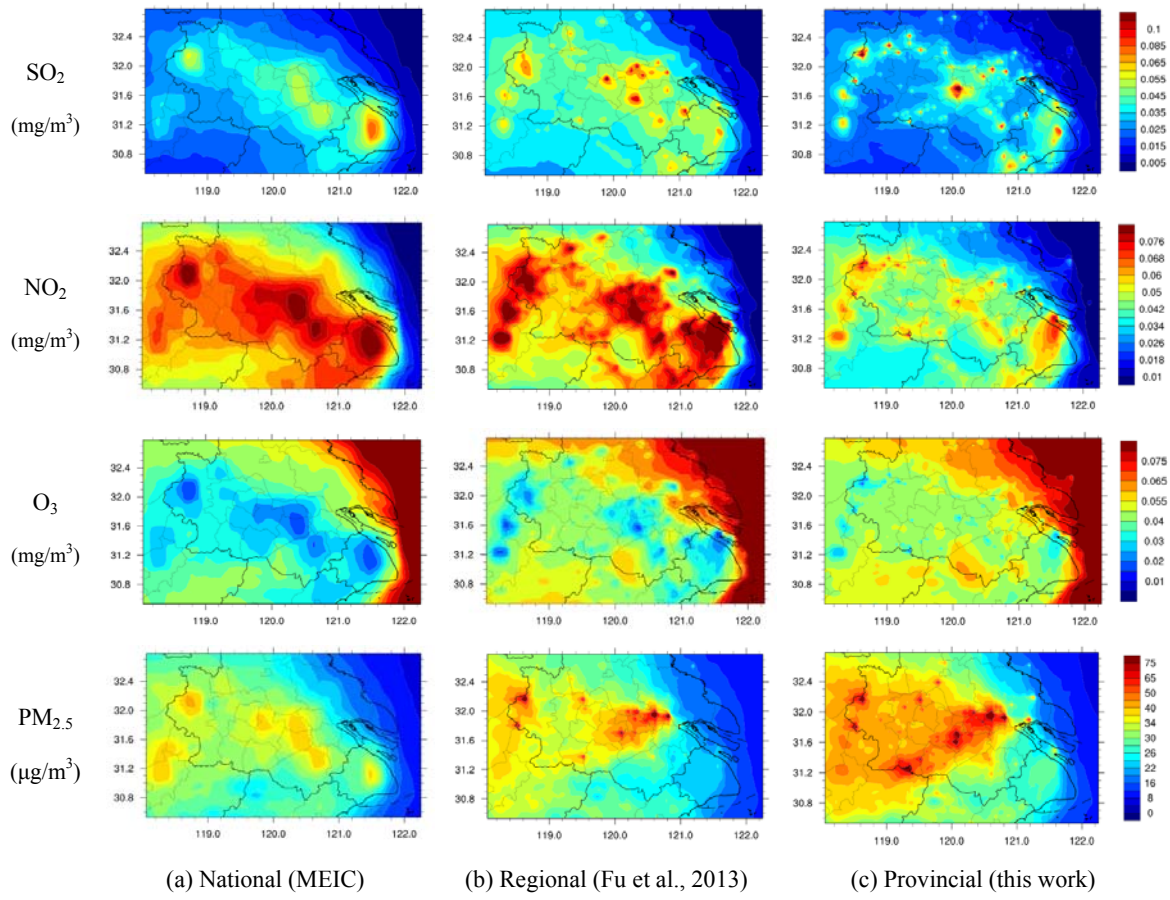


Figure 7

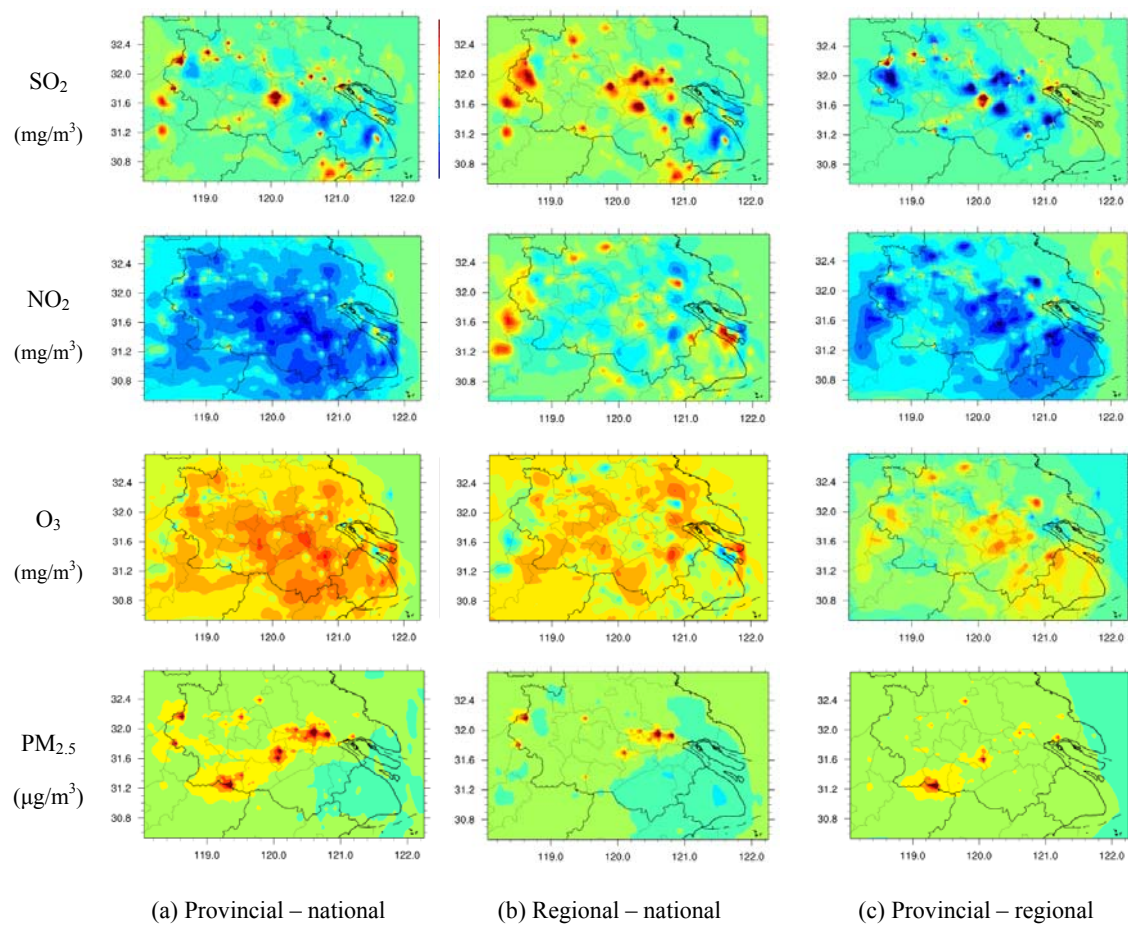


Figure 8

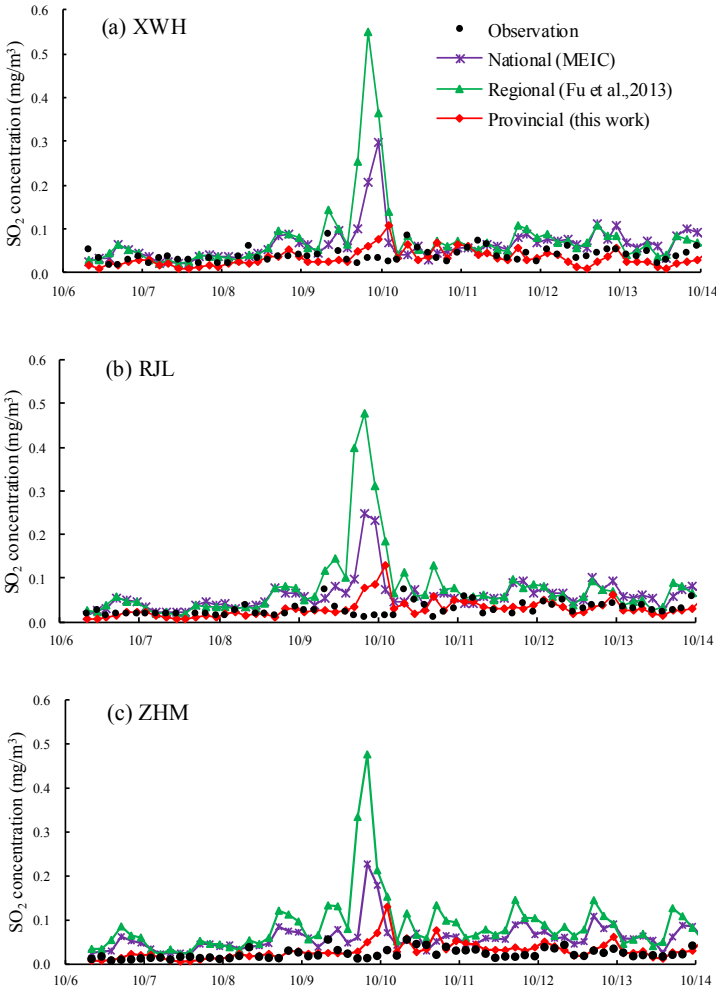


Figure 9

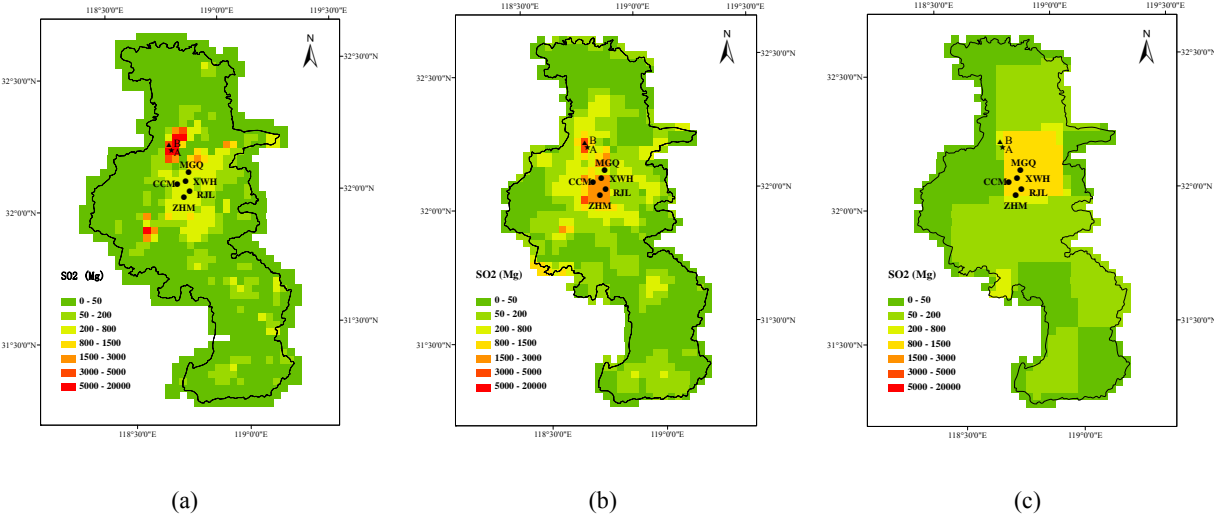
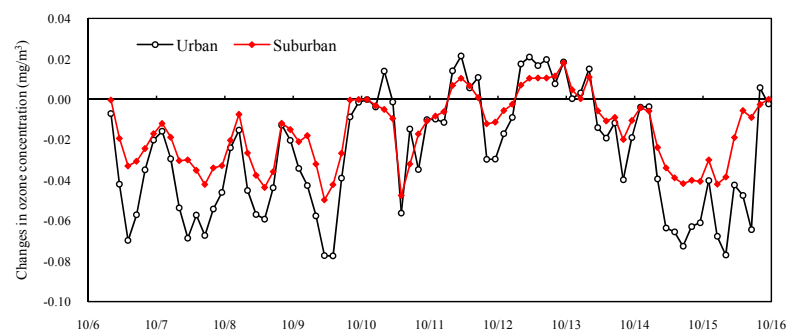
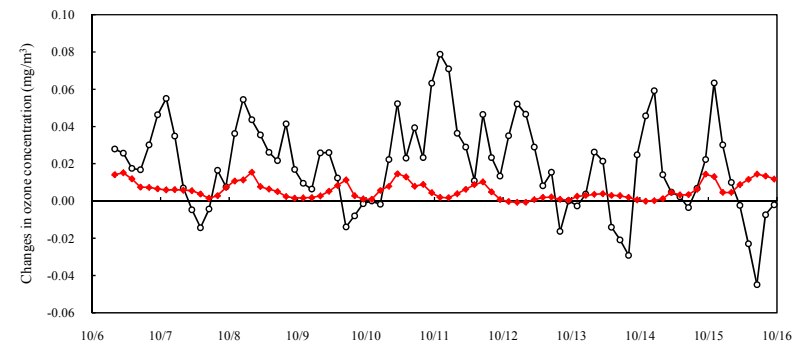


Figure 10



(a)



(b)